NASA CR70630

FEASIBILITY AND DESIGN STUDY:

ULTRAVIOLET DENSITY SENSOR

CALIBRATION FIXTURE

N66-18411

(ACCESSION NUMBER)

(THRU)

90

(PAGES)

1

(CODE)

CR 70630

(NASA CR OR TMX OR AD NUMBER)

23

(CATEGORY)

FACILITY FORM 602

GPO PRICE $ _____

CFSTI PRICE(S) $ _____

Hard copy (HC) $3.00

Microfiche (MF) .75

ff 653 July 65

Beckman®

023

Beckman®

STUDY OF THE FEASIBILITY AND DESIGN OF AN ULTRAVIOLET DENSITY SENSOR CALIBRATION FIXTURE

FINAL REPORT

Prepared by
Earl E. Miller

for

National Aeronautics and Space Administration
Flight Research Center

Contract NAS4-855

26 July 1965

Beckman® INSTRUMENTS, INC.
ADVANCED TECHNOLOGY OPERATIONS
FULLERTON, CALIFORNIA • 92634

TABLE OF CONTENTS

		Page
1.0	INTRODUCTION	1-1
2.0	THE ULTRAVIOLET DENSITY SENSOR	2-1
	2.0.1 Optical Design of the System	2-1
	2.0.2 Source Intensity	2-1
	2.1 Total Energy Rayleigh Scattered	2-2
	2.1.1 Scattering Volume	2-3
	2.1.2 Rayleigh's Scattering Cross Section	2-3
	2.2 Intensity Distribution Function for Rayleigh Scattering	2-4
	2.3 Fractional Energy Rayleigh Scattered into the Monochromator System	2-5
	2.4 Total Energy Rayleigh Scattered into the Monochromator System	2-6
	2.5 Extreme Values of Energy Incident Upon the Photocathode E_D	2-7
3.0	CALIBRATION FIXTURE FOR THE ULTRAVIOLET DENSITY SENSOR	3-1
	3.1 Signal to Noise Requirements	3-1
	3.2 Energy Levels of Reflected Stray Light	3-2
	3.2.1 A Single Reflection of Stray Light	3-3
	3.2.2 Trapping Reflected Stray Light	3-5
	3.2.3 Multiple Reflections of Stray Light	3-6
	3.3 Fresnel Diffraction	3-7
	3.4 Energy Levels of Fresnel Diffracted Stray Light Reflected from the Common Edge of T_S and T_D	3-8
	3.5 Reducing the Energy Levels of Fresnel Diffracted Stray Light Reflected from the Common Edge of T_S and T_D	3-9
	3.6 Optimizing the Position of $A_{S,1}$	3-12
	3.7 Locating the Outer Edges of T_S	3-12
	3.8 Attenuating the Energy Levels of Fresnel Diffracted Light Incident Upon $A_{D,o}$	3-13
	3.9 Selecting A Chamber Length	3-15
	3.10 Location of the Outer Edges of T_S in the 5.32 Meter Chamber	3-16
	3.11 Stopping and Trapping the FOV of the Focal Mirror and Detector	3-17
	3.12 Design of the Light Traps T_S and T_D	3-18
	3.13 Fraunhofer Diffraction	3-18

TABLE OF CONTENTS

	Page
3.14 Calibration Fixture Interior	3-20
3.15 Optical Paint	3-20
4.0 CONCLUSION	4-1
5.0 APPENDIX I	5-1
6.0 ILLUSTRATIONS	6-1
7.0 TABLE	7-1
8.0 BIBLIOGRAPHY	8-1

LIST OF ILLUSTRATIONS

Figure	Title	Page
I	Optical Diagram of the Ultraviolet Density	6-1
II	Optical Paths of the Source's Collimated Light I and the Collimated Rayleigh Scattered Light I_s	6-2
III	Intensity Distribution $F(\beta)$ of Light Rayleigh Scattered where, $F(\beta) = 1/2(1+\cos^2\beta)$	6-3
IV	Optical Path of the Ultraviolet Density Sensor	6-4
V	Optical Path of the 5.32 Meter Calibration Fixture (Folded Drawing)	6-5
VI	Fresnel Diffraction from a Straight Edge	6-6
VII	Reflectance of 3M Black Velvet Paint from 2500 to 3500 A	6-7
VIII	Cornu Spiral	6-8
Table I	Table of Fresnel Integrals and the Relative Intensities of Diffracted Light for Arc Length on the Cornu Spiral Ranging from 6 to 200 (folded table)	7-1

STUDY OF THE FEASIBILITY AND DESIGN OF

AN ULTRAVIOLET DENSITY SENSOR CALIBRATION FIXTURE

1.0 INTRODUCTION

This report presents the results of a study conducted at Beckman Instruments, Inc. for the National Aeronautics and Space Administration Flight Research Center for the purpose of mathematically investigating the design parameters of a calibration fixture for the ultraviolet density sensor. This study was conducted under National Aeronautics and Space Administration contract number NAS44855.

N66-8411

The study includes an analysis of the ultraviolet density sensor's optical paths and its detectable energy levels from Rayleigh scattering over an altitude range of 10 to 100 km. The optimum positions of aperture stops and light traps in the calibration fixture as well as the required number of aperture stops are determined for a signal-to-noise ratio of 100. A mathematical analysis of Fresnel and Fraunhofer diffraction of the aperture stops and multiple reflections in the light traps is also presented. A scale drawing has been made of the density sensor's optical path which shows the location of the aperture stops, light traps and scattering volume relative to the ultraviolet density sensor's instrument package.

2.0 THE ULTRAVIOLET DENSITY SENSOR

The ultraviolet density sensor measures the atmospheric air density in an altitude range of 10 to 100 km by monitoring the Rayleigh backscatter of an illuminated volume of the atmosphere.

2.0.1 Optical Design of the System

The optical components of the instrument are illustrated in Figure 1. An argon arc source is collimated by a parabolic collimating mirror and directed through the aperture stop $A_{s,2}$ and out of the instrument package. The centerlines of the source's collimated light beam and the detector monochromator's field of view (FOV) intersect 200 cm from the aperture stops $A_{s,2}$ and $A_{D,2}$ as shown in Figure II. The volume that is common to the source's beam and the detector monochromator's FOV defines the scattering volume. Light backscattered from the scattering volume that is directed toward the focal mirror of the detector system passes through the aperture stop $A_{D,2}$ and is focused on the entrance slit, S_p, of the Fery prism monochromator. The photocathode of a photomultiplier tube D, intercepts the light in the wavelength band of 1800 to 2800 A as passed by the monochromator.

2.0.2 Source Intensity

The argon arc source dissipates the energy stored in a .25 uf capacitor bank that is charged to a potential of 10,000 volts in 1 u sec. at a frequency of 2 cps. The resulting peak energy of each pulse is 10 megawatts. The amount of energy an argon arc radiates in the bandwidth $\Delta\lambda$ which extends from 1800 to 2800 A is approximately 9% of its total radiated energy over the bandwidth 1700 A to 1.4 microns.(1) Assuming at least 50% of the energy delivered to

the lamp is dissipated spectrally by the argon arc of radius a, the source's intensity B, over a unit sphere is given by

$$B = \frac{(10 \times 10^6 \text{ watts})\ (.09)\ (.5)}{(4\pi \text{ ster})\ (\Delta\lambda)\ \pi a^2}$$

The bandwidth ($\Delta\lambda$) from 1800 to 2800 A is 0.1 micron and the radius of the source 0.1 cm, therefore;

$$B = 1.14 \times 10^7 \ \frac{\text{watts}}{\text{stero-}\mu\text{-cm}^2} \qquad \text{I}$$

2.1 Total Energy Rayleigh Scattered

The energy density E that is incident upon the center of the scattering volume (Z-Z) where its cross sectional area is a maximum is given by

$$E = \frac{\pi B \sin^2\theta\ (\Delta\lambda)}{m^2} \ \text{watts/cm}^2 \qquad \text{II}$$

where,

2θ = median angle subtended by the source's collimating mirror.*

m = magnification of the source at the scattering zone (Z-Z').

For a parabolic reflector, the magnification m of an object a distance d from the reflector is approximately ℓ/d, where ℓ is the image distance.

In the UV density sensor, d and ℓ are the distances from the collimating mirror to the source and to the scattering zone (Z-Z) respectively. Hence, equation II may be written as

* The source's collimating mirror is rectangular, therefore; θ was determined for a circular mirror of equal area.

$$E = \pi B \sin^2\theta \, (\Delta\lambda) \, d^2/\ell^2 \text{ watts/cm}^2. \qquad \text{III}$$

The total amount of energy that will be scattered E_T by Rayleigh scattering in a volume V having a particle density N is given by

$$E_T = E N V \sigma_R \text{ watts} \qquad \text{IV}$$

where,

σ_R is the Rayleigh scattering cross section.

2.1.1 Scattering Volume

The scattering volume consists of two pyramids of approximately equal height h which have a common square base of length b. The scattering volume is, therefore; just twice the volume of a single pyramid or

$$V = 2/3 \, b^2 \, h \text{ cm}^3.$$

The density sensors pyramidal volume has a 7.94 cm base length b and an altitude h of 71 cm. These values yield a scattering volume of 2.98×10^3 cm^3.

2.1.2 Rayleigh's Scattering Cross Section

Rayleigh's scattering cross section for anisotropic particles that are small compared with the wavelength of the light being scattered is given by

$$\sigma_R = \frac{4\pi}{3} \left(\frac{2\pi}{\lambda}\right)^4 \alpha^2 \, \frac{6 + 3\rho_n}{6 - 7\rho_n} \text{ cm}^2 \qquad \text{V}^{(2)}$$

where,

α = polarizability of the scattering medium

ρ_n = depolarization factor of the molecular scatterers.

The depolarization factor is due to the anisotropy of the polarizability of

the molecules. The median depolarization factor for nitrogen as computed from several experimental values[3] is .0324. The polarizability of a model atmosphere[4] at 2400 A is approximately 1.93×10^{-24} cm^3 for the altitude range of 10 to 100 km. Substituting these values into V gives a Rayleigh cross section of

$$\sigma_R = \frac{4\pi}{3} \left(\frac{2\pi}{2.4 \times 10^{-5}}\right)^4 (1.93 \times 10^{-24})^2 \left[\frac{6 + 3\ (.0324)}{6 - 7\ (.0324)}\right]$$

or,

$$\sigma_R = 7.75 \times 10^{-26}\ cm^2.$$

The total amount of energy that is scattered from the scattering volume as a function of particle density is given from III and IV as

$$E_T^{(S)} = \pi B \sin^2\theta\ (\Delta\lambda)\ (d^2/\ell^2)\ N\ V \sigma_R. \qquad \text{VI}$$

2.2 Intensity Distribution Function for Rayleigh Scattering

Rayleigh scattering from a single scatterer has an intensity distribution in the plane of incidence which can be represented by the function $F(\beta) = 1/2\ (1 + \cos^2\beta)$ where, β is the scattering angle measured from the incident beam after it passes through the scattering center as illustrated in Figure III. This function limits the light intensity that is scattered at $\beta = \pi/2$ to one half the light intensity that is scattered at $\beta = 0$ or π. The energy E_c of of a light beam of intensity I that is uniformly distributed over an area A may be expressed as

$$E_c = I_o A.$$

The differential energy dE_c of a source of constant intensity is

$$dE_c = I_o dA.$$

For Rayleigh scattering, the intensity distribution takes on the form $I\,F(\beta)$, therefore;

$$dE_c = I \cdot 1/2(1 + \cos^2\beta)dA. \qquad \text{VII}$$

2.3 Fractional Energy Rayleigh Scattered into the Monochromator System

The energy E_c that is Rayleigh scattered over a sphere of radius R and into a cone $\beta = \pi \pm 0$ which fills the focal mirror of the monochromator, is given by integrating the differential energy dE_c over the area of the sphere that lies inside the cone. The integral of VII with limits of π and $\pi + \phi$ is

$$E_c = \int_{\pi}^{\pi+\phi} I \cdot 1/2(1 + \cos^2\beta)2\pi R^2 \sin\beta \, d\beta .$$

The total energy that is scattered over the sphere of radius R is given by integrating dE_c over the surface area of the sphere

$$E_T^{(s)} = \int_{0}^{\pi} I \cdot 1/2(1 + \cos^2\beta)2\pi R^2 \sin\beta \, d\beta .$$

The fractional amount of the total energy Rayleigh scattered that is received by the monochromator system is given by a ratio of $\frac{E_c}{E_T(s)}$ $E_T^{(s)}$, therefore;

$$E_c = \frac{\left| \pi R^2 I \int_{\pi}^{\pi+\phi} (1 + \cos^2\beta) \sin\beta \, d\beta \right|}{\left| \pi R^2 I \int_{0}^{\pi} (1 + \cos^2\beta) \sin\beta \, d\beta \right|} E_T^{(s)} .$$

Integrating gives

$$E_c = \frac{(\cos\beta + 1/3 \cos^3\beta)\Big|_{\pi}^{\pi+\phi}}{(\cos\beta + 1/3 \cos^3\beta)\Big|_{0}^{\pi}} E_T^{(s)} .$$

Evaluating E_c at the given limits,

$$E_c = 3/8(\cos\phi + 1/3\cos^3\phi - 4/3)\ E_T^{(s)}$$

since,

$$\cos(\pi + \phi) = -\cos\phi.$$

For small values of ϕ

$$\cos\phi \sim 1 - \phi^2/_2$$

and

$$\sin\phi \sim \phi,$$

therefore;

$$E_c = 3/8\ \phi^2\ E_T^{(s)}.$$

2.4 Total Energy Rayleigh Scattered into the Monochromator System

Since the collimating mirrors and focal mirrors have the same focal length and are equidistant from the scattering zone, $\ell/d \sin\phi = \sin\theta$ or $(\ell/d)\phi \simeq \sin\theta$ for small values of ϕ. The energy scattered into the detector monochromator's FOV for ϕ small is

$$E_c = \frac{3}{8}\frac{\sin^2\theta}{(\ell/d)^2}\ E_T^{(s)}. \qquad \text{VIII}$$

Substituting expression VI for the total energy scattered $E_T^{(s)}$ into VIII yields

$$E_c = 3/8\pi B \sin^4\theta\ (\Delta\lambda)\ d^4/\ell^4\ N\ V\ \sigma_R \text{ watts.} \qquad \text{IX}$$

The energy that is incident upon the photocathode of the photomultiplier tube E_D will be some fraction of the total energy Rayleigh scattered into the monochromator's FOV E_c due to absorption by the focal mirror and Fery prism. Assuming an optical efficiency Q of the monochromator system where Q is a ratio of the amount of energy incident upon its exit slit to that on its entrance slit, E_D may be expressed as

$$E_D = 3/8\pi B \sin^4\theta \ (\Delta\lambda) \ d^4/\ell^4 \ \sigma_R V \ QN. \qquad X$$

Evaluating X for an estimated monochromator efficiency of 60% in the 1800 to 2800 A bandwidth yeilds

$$E_D = 2.5 \times 10^{-24} \ N \text{ watts} \qquad XI$$

where,

$B = 1.14 \times 10^7$ watts/ster-u-cm^2

$\theta = 0.433$ radians

$\Delta\lambda = 0.1 \ \mu$

$d = 5.55$ cm

$\ell = 216$ cm

$V = 2.98 \times 10^3$ cm^3

$R = 7.75 \times 10^{-26}$ cm^2

$Q = 0.6$

2.5 Extreme Values of Energy Incident Upon the Photocathode E_D

The ultraviolet density sensor is designed to measure the particle density of the atmosphere in an altitude range of 10 to 100 km. Since the particle density N of the atmosphere is directly proportional to the altitude, the range of E_D will be evaluated with representative values of N[5] at the altitude extremes of 10 and 100 km. At 10 km and 100 km, the particle density is 8.6×10^{18} and 7.8×10^{12} particle/cm^3 respectively. Evaluating E_D at these extreme altitudes gives

$$\left.\begin{aligned} E_D &= 2.15 \times 10^{-5} \text{ watts at 10 km} \\ &\text{and} \\ E_D &= 1.95 \times 10^{-11} \text{ watts at 100 km.} \end{aligned}\right\} \ XII$$

The energy E_q of a quanta having a wavelength of 2400 A is 8.25×10^{-19} watt-sec. Incidence rates of quanta on the photomultiplier tubes photocathode is given by

$$E_D/E_q.$$

Using the values of E_D given in XII, the extreme rates are

2.6×10^{13} quanta/sec. at 10 km

and

2.36×10^{7} quanta/sec. at 100 km.

3.0 CALIBRATION FIXTURE FOR THE ULTRAVIOLET DENSITY SENSOR

The ultraviolet density sensor must be calibrated in a vacuum chamber which simulates the atmosphere over an altitude raten of 10 to 100 km. Detection of the energy Rayleigh scattered into the monochromator system of the density sensor with a signal to noise ratio S, places a limiting requirement on the energy level of the unwanted stray light that may enter the monochromator. Assuming all stray light originates from scattering on the surface of the density sensor's collimating mirror and fused silica window, the vacuum chamber must be designed such that a given S is satisfied over the 10 to 100 km altitude range.

3.1 Signal to Noise Requirements

The energy Rayleigh scattered into the monochromator system is a minimum at an altitude of 100 km. The energy incident upon the photocathode of the density sensors photomultiplier tube at this altitude is given by

$$E_D = 3/8\,\pi B \sin^4\theta\,(\Delta\lambda)\,(d^4/\ell^4)\,\sigma_R\,V\,Q\,N \qquad \text{X}$$

evaluated at 100 km or

$$E_D(100\text{ km}) = 3/8\,\pi B \sin^4\theta\,(\Delta\lambda)\,(d^4/\ell^4)\,\sigma_R\,VQN(100\text{ km}) \qquad \text{XIII}$$

where,

N(100 km) = particle density of the atmosphere at an altitude of 100 km.

If the signal to noise ratio is S, the maximum amount of energy which falls on the detector E_m due to stray light is

$$E_m = (1/S)E_D\,(100\text{ km}) \qquad \text{XIV}$$

It is required that E_m be smaller than E_D and the value of S be substantially larger than one.

3.2 Energy Levels of Reflected Stray Light

Consider the energy level of light scattered from the surface of the collimating mirror after n reflections from i surfaces each having reflectance R_i. If the source's beam travels a distance L_i between reflecting surfaces where,

L_o = distance from the collimating mirror to the first surface

L_1 = distance from the first to the second surface

L_2 = distance from the second to the third surface

L_n = distance from the nth surface to the focal mirror

the energy density of reflected light $E_{r,n}$ in the bandwidth $\Delta\lambda$ that is incident upon the focal mirror after n reflections is given by

$$E_{r,n} = Q'\pi B \sin^2\theta\ (\Delta\lambda)\ R_i^n d^2 \left(L_o + \sum_{i=1}^{n} L_i \right)^{-2} \prod_{i=1}^{n} \frac{\Omega_{i+1}}{\Omega_i} \qquad \text{XV}$$

where,

Ω_i = total solid angle subtended by the light reflected from the ith surface*

Ω_{i+1} = solid angle the i+1 surface subtends from the ith surface

Q' = fractional source energy scattered by the collimating mirror.

The reflected energy $E_{R,n}$ that is incident upon the photocathode of the monochromator's photomultiplier tube is given by

* If the ith surface is a plane, the reflected light would have a hemispherical distribution and Ω_o would equal 2π.

$$E_{R,n} = E_{r,n} \; Q \; A_m \qquad \text{XVI}$$

where,

A_m = area of the focal mirror

Q = optical efficiency of the monochromator system.

Combining XV and XVI gives

$$E_{R,n} = Q \; Q' \; A_m \pi B \sin^2\theta \; (\Delta\lambda) R_i^n \; (d^2/L^2) \prod_{i=1}^{n} \frac{i+1}{i} \qquad \text{XVII}$$

where,

L = total pathlength of the stray light = $L_o + \sum_{i=1}^{n} L_i$.

But $E_{R,n}$ must be less than or equal to E_m to satisfy the noise requirements. This may be expressed mathematically by

$$E_{R,n} \leq E_m. \qquad \text{XVIII}$$

Combining XIII and XIV, XVIII may be expressed as

$$Q \; Q' \; A_m \pi B \sin^2\theta \; (\Delta\lambda) R_i^n (d^2/L^2) \prod_{i=1}^{n} \frac{\Omega_{i+1}}{\Omega_i}$$

$$\leq \frac{1}{S} \frac{3}{8} \pi B \sin^4\theta \; (\Delta\lambda)(d^4/\ell^4) \; \sigma_R \; V \; Q \; N \; (100 \text{ km}).$$

Cancelling terms,

$$\frac{R_i^n}{L^2} = \frac{3}{8} \frac{\sin^2\theta}{S A_m Q'} \frac{d^2}{\ell^4} \sigma_R \; V \prod_{i=1}^{n} \frac{\Omega_i}{\Omega_{i+1}} \; N(100 \text{ km}). \qquad \text{XIX}$$

3.2.1 A Single Reflection of Stray Light

For a single reflection from a region on a planar surface that is equidistant from the collimating and focal mirrors,

$$\frac{R_1}{L^2} \leq \frac{3}{8} \frac{\sin^2\theta}{SA_mQ'} \frac{d^2}{\ell^4} \sigma_R V \frac{\Omega_1}{\Omega_2} N (100 \text{ km}).$$

where,

$L/2$ = distance from the reflecting surface to the focal mirror

Ω_1 = total solid angle subtended by the reflected light

Ω_2 = solid angle subtended by the focal mirror from the reflecting surface.

Ω_2 may be expressed as

$$\Omega_2 = \frac{A_m}{(L/2)^2}$$

and

$$\Omega_1 = 2\pi,$$

therefore,

$$\frac{R_1}{L^4} \leq \frac{3\pi}{16} \frac{\sin^2\theta}{S\ Q'\ A_m^2} \frac{d^2}{\ell^4} \sigma_R V N (100 \text{ km}).$$

The total path length that is required to reduce the energy of the stray light to an acceptable noise level is given by

$$L \geq \left[\frac{16}{3\pi} \frac{S\ Q'\ A_m^2 \ell^4 R_1}{\sin^2\theta\ d^2\ \sigma_R\ N(100 \text{ km})}\right]^{1/4} \qquad \text{XX}$$

where, the stray light has undergone a single reflection. Evaluating XX for a 5 cm square focal mirror and a reflectance of .05 gives

$$L \geq 1.3 \times 10^4 \text{ meters}$$

where,

S = 100

Q' = 0.25

$A_m = 25\ cm^2$

$\ell = 216\ cm$

$R_1 = .05$

$\theta = 0.433$ radians

$d = 5.55\ cm$

$\sigma_R = 7.75 \times 10^{-26}\ cm^2$

$N(100\ km) = 7.8 \times 10^{12}\ cm^{-3}$

This prohibitively large value of L requires that the extended energy of the source be trapped in a region that lies out of the FOV of the monochromator as illustrated in Figure IV.

3.2.2 Trapping Reflected Stray Light

Since the collimating and focal mirrors are potential scatterers with FOV's which include and are greater than the source's and monochromator's FOV's respectively (see Figure IV), the source's light trap T_s must include all of the collimating mirror's FOV and still be isolated from the FOV of the focal mirror. To be certain that the FOV of the focal mirror is optically black, a light trap T_D must terminate it also.

Isolation of the collimating and focal mirror's FOV's as illustrated in Figure IV would obviously occur at some prohibitive distance from the aperture $A_{s,2}$ and $A_{D,2}$ which would also result in a prohibitively large value of L. The placement of rectangular apertures $A_{s,k}$ and $A_{D,k}$ where k = 1,2 and a straight edge $A_{s,o}$ and $A_{D,o}$ along the FOV of the source and monochromator respectively as illustrated in Figure IV, reduces the FOV's of the collimating and focal mirrors to a minimum without interfering with the scattering volume.

Figure V (a folded drawing) is a scale drawing of the optical paths of the UV density sensor. The collimating mirror's FOV is restricted by the aperture stops $A_{s,o}$, $A_{s,1}$ and $A_{s,2}$. Likewise, $A_{D,o}$, $A_{D,1}$ and $A_{D,2}$ define the focal mirrors FOV. These two FOV's are isolated from each other at the point P. The distance from P to the scattering region (Z-Z) is approximately 280 cm. P' is located at a point where the FOV's are separated by 1.25 cm and (Z-Z)P' is approximately 316 cm. The opening of the light traps T_s and T_D are placed at P' such that they have a common edge as shown.

The fractional source energy that will be scattered by the fused silica window will be less than 10% of that which is scattered by the collimating mirror, therefore; its contribution to the unwanted stray light is assumed to be negligible.

3.2.3 Multiple Reflections of Stray Light

Assuming that a light beam entering T_s travels a distance of 100 cm while encountering n reflections, the total pathlength L would, therefore; be

$$L = 2\ (532) + 100 = 1164 \text{ cm.}$$

The minimum number of reflections that are required in T_s to reduce the reflected energy $E_{R,n}$ to some value that is less than or equal to E_m is given by

$$\frac{R_1^n}{L^2} \leq \frac{3}{8}\ \frac{\sin^2\theta}{SA_m\ Q'}\ \frac{d^2}{\ell^4}\ \sigma_R\ V\ \prod_{i=1}^{n}\left(\frac{\Omega_i}{\Omega_{i+1}}\right)\ N\ (100 \text{ km}) \qquad \text{XIX}$$

evaluated with L equal to 1164 cm.

Assuming all of the light that is reflected in T_s remains in T_s until the final or $n^{\underline{th}}$ reflection

$$\prod_{i=1}^{n} \frac{\Omega_i}{\Omega_{i+1}} = \frac{\Omega_n}{\Omega_{n+1}}$$

where,

Ω_n = solid angle subtended by the light reflected from the nth surface

Ω_{n+1} = solid angle subtended by the focal mirror from the nth surface.

For a uniform reflectance of .05 in T_s and assuming the nth surface is planar and located a distance L/2 from the focal mirror, XIX may be written as

$$(.05)^n \quad \frac{3}{8} \; \frac{\sin^2\theta}{S\,Q'} \; \frac{d^2}{4} \quad R\,V\,\frac{2}{A^2_m} \quad L^4\,N(100\text{ km}). \qquad \text{XXI}$$

Evaluating XXI yields

$$(.05)^n \leq 1 \times 10^{-10},$$

therefore,

$$n \geq 9.$$

Thus, nine or more reflections of the stray light scattered from the collimating mirror will attenuate its energy to the acceptable noise level in the case where the beam travels a total distance of 100 cm while inside T_s. Attenuation of the source's collimated light beam would require ten or more reflections. This may be found by setting Q' equal to one in XXI.

The energy of all light at the edge of the light trap T_s which is common to both T_s and T_D must also be investigated.

3.3 Fresnel Diffraction

There is associated with each aperture stop some Fresnel diffraction of the stray light leaving the surface of the collimating mirror, since each side of the rectangular stop is analagous to a straight edge. Figure VI

illustrates a light beam of intensity I_o and wavelength λ that is incident upon a straight edge which lies a distance f from a point source. The relative intensity of the light I/I_o falling on the screen a distance h from the straight edge is a function of its vertical distance S above or below the straight edge and is given in Figure VIII by the Cornu spiral.[6] The function which yields the distance v to be measured along the spiral is

$$v = S\sqrt{\frac{2(f+h)}{fh}}$$

where, S is the arc distance of the light beam above the straight edge. For $S < 0$, the relative intensity I/I_o is directly proportional to v. If $y << f + h$, v may be expressed as

$$v = \frac{fy}{f+h}\sqrt{\frac{2(f+h)}{fh}} \quad . \qquad \text{XXII}$$

The relative intensity along the edge of the collimated beam where y = o (therefore, v = o also) is 0.25 I/I_o independent of the distance f and h and the wavelength of the light being diffracted.

3.4 Energy Levels of Fresnel Diffracted Stray Light Reflected from the Common Edge of T_s and T_D

The source light beam is collimated by three aperture stops $A_{s,o}$, $A_{s,1}$ and $A_{s,2}$ as illustrated in Figure V. But, the collimating mirror's FOV is restricted by the aperture stops $A_{s,o}$ and $A_{s,1}$. To determine the relative intensity of diffracted stray light at the edge that is common to T_s and T_D requires computing $(I/I_o)_{A_{s,o}}$ for a given distance y_o. The distance y_o in this case is the distance from the edge of the collimating mirror's FOV to the common edge of T_s and T_D. $A_{s,o}$ is located 194 cm from the collimating

mirror and 338 cm from the edge that is common to the light traps T_s and T_D.

Evaluating XXII for f_o = 192 cm, h_o = 340 cm and a maximum wavelength of 2800 A at y_o gives

$$v = -(8.75)\ y_o. \qquad \text{XXIII}$$

This value of v, when applied to the Cornu spiral will yield a relative intensity at the common edge of T_s and T_D due to the diffraction effects of $A_{s,o}$.

The net relative intensity of the source beam at the common edge of T_s and T_D due to Fresnel diffraction is, therefore;

$$\left(\frac{I}{I_o}\right)_{A_{s,o}}. \qquad \text{XXIV}$$

The general expression of the energy E_e of the source's beam which may be incident upon the photomultiplier tube photocathode after a single reflection from the common edge of T_s and T_D is given by the product of XVII and XXIV as,

$$E_e = Q\ Q'\ A_n \pi\ B \sin^2\theta\ (\Delta\lambda)\ \frac{d^2}{L^2}\ R\ \frac{\Omega_2}{\Omega_1}\left(I/I_o\right)_{A_{s,o}}.$$

3.5 <u>Reducing the Energy Levels of Fresnel Diffracted Stray Light Reflected from the Common Edge of T_s and T_D</u>

The energy level of diffracted light that is incident upon the photocathode of the photomultiplier tube must be less than or equal to the maximum allowable energy level of incident stray light.

$$E_e \leq E_m,$$

therefore;

$$Q\ Q'\ A_m\ \pi\ B\ \sin^2\theta\ (\Delta\lambda)\ \frac{d^2}{L^2}\ R\ \frac{\Omega_2}{\Omega_1}\left(I/I_o\right)_{A_{s,o}}$$

$$\leq \frac{3}{8}\frac{\pi}{S}\ B\ \sin^4\theta\ (\Delta\lambda)\ \frac{d^4}{\ell^4}\ \sigma_R\ V\ Q\ N\ (100\ \text{km}).$$

Cancelling terms and solving for the relative attenuation due to Fresnel diffraction yields

$$(I/I_o)_{A_{s,o}} \leq \frac{3}{8}\frac{\sin^2\theta}{S}\ \frac{d^2}{\ell^4}\ \frac{\sigma_R\ V\ N(100\ \text{km})}{A_m\ R\ Q'}\ L^2\ \frac{\Omega_1}{\Omega_2}\ . \qquad \text{XXV}$$

The solid angle the focal mirror subtends Ω_2 from the common edge of T_s and T_D is $A_m/(L/2)$, therefore, XXV may be simplified to

$$(I/I_o)_{A_{s,o}} \leq \frac{3}{8}\frac{\sin^2\theta}{S}\ \frac{d^2}{\ell^4}\ \frac{\sigma_R\ V\ N\ (100\ \text{km})}{A_m^2\ R\ Q'}\ L^4\Omega_1\ . \qquad \text{XXV}$$

Evaluating XXV gives

$$(I/I_o)_{A_{s,o}} \leq 1.5 \times 10^{-20}\ L^4 \qquad \text{XXVI}$$

where,

$$\Omega_1 = 2\pi \text{ steradians}$$

$$(I_o/I)_{A_{s,o}} = (8.6 \times 10^{-2})^{-1}$$

$$R = .05$$

$$d = 5.55 \text{ cm}$$

$$\ell = 216 \text{ cm}$$

$$N(100\ \text{km}) = 7.8 \times 10^{12}\ \text{cm}^{-3}$$

$$\theta = .446 \text{ radians}$$

$$A_m = 25\ \text{cm}^2$$

$$R = 7.75 \times 10^{-26}\ \text{cm}^2$$

$$V = 2.98 \times 10^3\ \text{cm}^3$$

$$S = 100$$

Examining the case where the aperture of T_s is located a distance of 532 cm from the plane of the mirrors, $(I/I_o)_{A_{s,o}}$ must be less than or equal to 1.9×10^{-8}.

For this case, y_o must be less than or equal to -1.77 cm which is the total separation of the FOV of the two mirrors at P'. Inserting the maximum value of y_o into XXIII yields a value for the arc length on the Cornu spiral of

$$v = -15.5.$$

The relative attenuation of the Fresnel diffracted stray light at the common edge of T_s and T_D which is coincident with the edge of the focal mirror's FOV at $y_o = -1.77$ is

$$(I/I_o)_{A_{s,o}} \simeq 2.1 \times 10^{-4}. \qquad \text{XXVII}$$

The attenuation of the diffracted light is therefore inadequate at $y_o = -1.27$ cm.

The energy of diffracted stray light reflected from the common edge of T_s and T_D may be reduced by increasing the distance from the aperture of T_s and T_D and the plane of the mirrors L/2. The slope of the divergence of the inner edges of the FOV of the two mirrors beyond their intersection point P (see Figure V) is 1/70. Increasing the distance between the light traps and the mirrors such that L is 3150 cm, the value of y_o must now be,

$$y_o \leq (3150/2 - 35)\ 1/70 = 22 \text{ cm}$$

since, the distance from P to P' is 35 cm. Inserting the maximum value of y_o into XXIII gives an arc length on the Cornu spiral of

$$v = 192.$$

The relative attenuation of the diffracted stray light is now

$$(I/I_o)_{A_{s,o}} \simeq 1.37 \times 10^{-6}.$$

Inserting the new value of L into XXVI yields

$$(I/I_o)_{A_{s,o}} \leq (1.5 \times 10^{-20})\ (3.15 \times 10^3)^4 = 1.48 \times 10^{-6}.$$

Thus, the calibration fixture must be housed in a 15.75 m long vacuum chamber (excluding the light traps T_s and T_D). The chamber may be shortened if the common edge of T_s and T_D is extremely sharp and T_D sufficiently attenuates all diffracted stray light which enters its aperture.

3.6 Optimizing the Position of $A_{s,1}$

The relative attenuation of $A_{s,1}$ is dependent upon y_1 and the distance f_1 and h_1 from $A_{s,1}$ to the collimating mirror and to T_s respectively. Since it is desirable to keep the aperture of T_s as small as possible, the position of $A_{s,1}$ must be chosen such that the required distance from the outer edges of the collimating mirrors FOV to its respective outer edge of T_s is a minimum. An examination of XXII for the three cases $f \ll h$, $f = h$ and $f \gg h$ shows that v will be a maximum when $f \gg h$.

The optimum position of $A_{s,1}$ would, therefore, be as near to the scattering zone as is physically possible. Positioning $A_{s,1}$ where the distance between the sources and the detectors collimated beams is .635 cm yields values of f_1 and h_1 of 138 cm and 394 cm respectively.

3.7 Locating the Outer Edges of T_s

The energy of stray light that is diffracted by $A_{s,1}$ and reflected from the

outer edges of T_s may be treated in the same manner as was the edge common to T_s and T_D. Since the distance from the mirrors to the outer edges of T_s has been established in Section 3.5, the required distance y of the outer edges of T_s from their respective edges of the collimating mirror's FOV must be determined. XXVI evaluated at

$$L = 3150 \text{ cm.}$$

gives

$$(I/I_o)_{A_{s,1}} \leq 1.48 \times 10^{-6}.$$

This relative intensity requires an arc length on the Cornu spiral of

$$v = 185.$$

$A_{s,1}$ is located 138 cm from the collimating mirror and 1437 cm from the aperture of T_s. Evaluating XXII and solving for y gives

$$y = 83.5 \text{ cm}$$

where,

$f = 138$ cm

$h = 1437$ cm

$v = 18$

$\lambda = 2800$ A.

3.8 Attenuating the Energy Levels of Fresnel Diffracted Light Incident Upon $A_{D,o}$

The sources beam is collimated by the aperture stops $A_{s,1}$ and $A_{s,2}$ before entering the scattering volume (see Figure V). The collimated beam will be diffracted onto aperture stop $A_{D,o}$ by $A_{s,1}$. The required relative intensity of the diffracted light that is incident upon the surface of $A_{D,o}$ and

reflected into the focal mirror's FOV is given by XXVI generalized for n aperture stops in the source's beam

$$\prod_{k=1}^{n} (I/I_o)_{A_{s,k}} \leq 1.5 \times 10^{-20} L^4. \qquad \text{XXVIII}$$

The diffraction term may be separated into two terms

$$\prod_{k=2}^{n} (I/I_o)_{A_{s,k}} \quad (I/I_o)_{A_{s,1}} \leq 1.5 \times 10^{-20} L^4 \qquad \text{XXIX}$$

since, $A_{s,k}$, where k = 2,3, ..., n collimates the beam and yields a relative intensity of the source beam of 0.25 along y = o. $A_{s,1}$ diffracts the energy incident upon it onto $A_{D,o}$ a distance y from the edge of the source's beam with a relative intensity that may be found from the Cornu spiral.

Evaluating the arc length from

$$v = \frac{y_1 f_1}{f_1 + h_1} \sqrt{\frac{2 (f_1 + h_1)}{f_1 h_1}} \qquad \text{XXII}$$

where,

y_1 = -2.22 cm

f_1 = 138 cm

h_1 = 53.8 cm

λ = 2800 A

v = -69.

Therefore,

$$(I/I_o)_{A_{s,1}} = 1.06 \times 10^{-5}$$

Inserting this into XXIX along with the attenuation of the n-1 aperture stops located along the source's beam between $A_{s,1}$ and $A_{s,2}$ and including $A_{s,2}$ gives

$$(0.25)^n \leq 3 \times 10^{-5} \qquad \text{XXX}$$

where,

$$L = 2\ (f_1+h_1) = 383.6 \text{ cm.}$$

Evaluating XXX,

$$n \geq 8.$$

Thus, seven aperture stops are needed between $A_{s,1}$ and $A_{s,2}$ (as illustrated in Figure V) to reduce the intensity of the Fresnel diffracted stray light reflected from the inner edge of $A_{D,o}$ to the minimum acceptable noise level at the photocathode.

3.9 Selecting a Chamber Length

The 15.75 meter long chamber is required if the Fresnel diffracted stray light undergoes a single reflection from the common edge of T_s and T_D in its total path between the collimating and focal mirrors.

Examining the 5.32 meter chamber illustrated in Figure V shows that the common edge of T_s and T_D is out of the focal mirror's FOV, therefore, stray light reflected from it must undergo more than one reflection to fall upon the focal mirror. Evaluating XXV for the case of n reflections

$$(I/I_o)_{A_{s,o}} \leq 1.5 \times 10^{-20} \frac{L^4}{(.05)^n} \qquad \text{XXXI}$$

The relative attenuation of Fresnel diffracted stray light by $A_{s,o}$ at the common edge of T_s and T_D is 2.1×10^{-4} as given by XXVII.

Evaluating XXXI for the 5.32 meter chamber and solving for the required number of reflections gives

$$(.05)^n \leq .915 \times 10^{-4},$$

therefore;

$$n \geq 4.$$

Thus, a total of four reflections of the Fresnel diffracted stray light which falls upon the common edge of T_s and T_D will attenuate it to the acceptable noise level. To insure multiple reflections of stray light entering the focal mirror's FOV, aperture stops should be provided between $A_{D,1}$ and $A_{D,2}$ as shown on Figure V. The exact number of required stops will depend on the cross sectional area of the chamber and must be determined experimentally.

Fresnel diffracted stray light will also enter the aperture of the focal mirror's light trap T_D in the 5.32 meter chamber. If the geometric configuration of the light trap is such that the angle of incidence of stray light falling upon it is low, the trap should remain sufficiently black.

3.10 Location of the Outer Edges of T_s in the 5.32 Meter Chamber

The location of the outer edges of T_s is solely dependent upon the maximum allowable energy level E_m of Fresnel diffracted stray light that may be reflected from it. The energy level that is reflected from the outer edges E_o is dependent upon the distance y_1 from the outer edges of the collimating mirror's FOV to their respective edge of the light trap T_s. Since y_1 may take on any value, it must be found from the inequality

$$(I/I_o)_{A_{s,1}} \leq 1.5 \times 10^{-20} L^4. \qquad \text{XXVI}$$

For a 5.32 meter chamber

$$(I/I_o)_{A_{s,1}} \leq 1.9 \times 10^{-8}$$

since,

$$L = 1064 \text{ cm.}$$

This relative intensity requires an arc length on the Cornu spiral of

$$v > 200.$$

This would require a separation between the outer edges of the collimating mirror's FOV and their respective edges of T_s of

$$y > 36 \text{ cm.}$$

The outer edges of the source's light trap T_s is out of the FOV of the focal mirror, therefore, the assumption that a single reflection of the Fresnel diffracted stray light from its edge will cause it to fall upon the focal mirror is false. The required number of reflections of the stray light after being reflected from the outer edge may be determined from XXXI

$$(I/I_o)_{A_{s,1}} \leq (1.5 \times 10^{-20}) \frac{L^4}{(.05)^n} .$$

In this case, however, the optimum distance between the outer edges of T_s and the collimating mirror's FOV must be used to evaluate the relative attenuation of the Fresnel diffracted stray energy at the edges. Also, L would have the value of 1064 cm for the 5.32 meter chamber. Hence

$$(.05)^n \leq (1.9 \times 10^{-8}) (I/I_o)^{-1}_{A_{s,1}} .$$

3.11 <u>Stopping and Trapping the FOV of the Focal Mirror and Detector</u>

Because of the symmetry of the focal and collimating mirror's FOV, the focal mirror's FOV and the monochromator's FOV may be treated in the same manner as the sources. The apertures $A_{D,q}$ where q = 0, 1, ..., 9 are primarily for

the restriction of the focal mirror's FOV. It is also necessary to place other apertures a_s and a_o along the FOV of the two mirrors as illustrated in Figure V to prevent the generation of stray light along the walls of the calibration fixture by reflection. These apertures need not contribute to the collimation of the FOV's or attenuation of diffracted light. The apertures a_s trap the stray light which may originate from the scattering in the source's envelope or housing. Stray light entering the detectors leading apertures $A_{D,3}$ or $A_{D,4}$ at angles other than those which are coincident with the FOV of the focal mirror will likewise be attenuated by a_D. Their number and spacing is dependent upon the calibration fixtures physical size as was mentioned in Section 3.9.

3.12 Design of the Light Traps T_s and T_D

The Rayleigh horn is recommended for the light traps T_s and T_D. Figure IV illustrates the optical paths of the calibration fixture with the Rayleigh horn light traps. The interior surface of the horn must be smooth. Also, T_s must be free of any macroscopic disfigurations which may scatter stray light into the system.

3.13 Fraunhofer Diffraction

The aperture nearest the collimating mirror, $A_{s,2}$ also diffracts the source's collimated beam by Fraunhofer diffraction. The intensity distribution of Fraunhofer diffraction is given by

$$I \sim \frac{\sin^2\left(\frac{\pi b \sin\alpha}{\lambda}\right)}{\left(\frac{\pi b \sin\alpha}{\lambda}\right)}$$

where,

b = length of one side of the square aperture $A_{s,2}$

λ = wavelength of the source's beam

α = angle subtended from the center of the aperture to a point on a screen where the central ray's intensity is I.

The angle subtended from the central maxima to the first minima of the Fraunhofer diffraction pattern is given by

$$\frac{\pi b \sin \alpha}{\lambda} = \pi,$$

therefore,

$$\alpha = \sin^{-1} \frac{\lambda}{b} .$$

Evaluating the maximum value of α for an extreme wavelength of the density sesnor's bandwidth gives

$$\alpha = 5.6 \times 10^{-6} \text{ radians}$$

where,

λ = 2800 A

b = 5 cm.

The length w of the central maxima at the entrance to T_s is given by

$$w = 2\alpha (a/2) = \alpha a$$

where, a/2 is the distance from the collimating mirror to the entrance of T_s.

Evaluating w for the 5.32 m chamber;

$$w = 2.9 \times 10^{-3} \text{ cm}$$

where,

a = 532 cm.

The width of the aperture of T_s is greater than 18 cm, therefore, Fraunhofer

diffraction effects are negligible in the 5.32 m calibration fixture.

3.14 Calibration Fixture Interior

It is important that the edges of all apertures and especially the common edge of T_S and T_D be as sharp as is possible. Also, the total interior of the calibration fixture including its light traps and apertures must be coated with an optically black paint that will insure a reflectance that is less than or equal to .05 in the 1800 to 2800 A bandwidth.

3.15 Optical Paint

A paint recommended for the calibration chamber is the Minnesota Manufacturing and Mining Company's "velvet coating." This paint has a reflectance which ranges from .01 to .05 at angles up to 70° from the coated surface's normal. Its maximum reflectance at grazing incidence is 0.17. Calculations in this report are based on a reflectance of .05, which is a generous figure since the incident angles of all light in the collimating mirrors FOV excluding T_S is near zero. Figure VII shows the reflectance of this paint in the wavelength range of 2500 to 3600 A where the angle of incidence is 5°.

The calibration fixture must be evacuated to 10^{-4} torr to simulate conditions at 100 km. Velvet coating will easily satisfy these vacuum requirements. Its manufacturer reports a 1% weight loss for velvet coating after 7 days in a vacuum of 4.5×10^{-8} torr at room temperature.

4.0 CONCLUSION

The required length L/2 of the calibration fixture's vacuum chamber for adequate attenuation of stray light scattered from the surface of the collimating mirror and the fused silica exit window is dependent primarily upon the scattering coefficient Q' of the collimating mirror assuming the exit window's contribution is negligible, the number of refelctions n of the stray light from surfaces within the fixture having a reflectance R and the relative attenuation of the stray light Fresnel diffracted by $A_{s,o}$ $(I/I_o)_{A_{s,o}}$ onto the common edge of the source's and detector's light traps T_s and T_D respectively. The relationship between these factors is shown by evaluating XXV in terms of Q', n, R and $(I/I_o)_{A_{s,o}}$ for the general case of n reflections

$$L \geq \left[(2.66 \times 10^{20})\ Q'\ R^n\ (I/I_o)_{A_{s,o}}\right]^{1/4}.$$

If the scattering coefficient of the collimating mirror is zero, the only requirement of the calibration fixture would be to trap the source's collimated beam and its length would be defined by the distance to the point of separation of the FOV of the two mirrors. Also, since $R < 1$, a large number of reflections will relax the requirements of L. But $(I/I_o)_{A_{s,o}}$ is inversely proportional to L, therefore, a compromise must be made between the number of reflections the stray light scattered from the collimating mirror of given Q' must encounter before falling upon the focal mirror and the length L/2 of the calibration fixture's vacuum chamber.

A single reflection of the stray light from the common edge of T_s and T_D requires a chamber length of 15.75 meters. Increasing the number of reflections to a total of four allows a reduction in the chamber's length to

5.32 meters. It is recommended that the 5.32 meter chamber as illustrated in Figure V be fabricated, since all reflecting surfaces lie out of the monochromator's FOV with the exception of the light trap T_D. Stray light entering the Rayleigh horn trap T_D will be incident upon its surface at near grazing incidence and therefore be attenuated by multiple reflections in its tip.

The energy level of stray light produced by the ultraviolet density sensor can be attenuated in the 5.32 meter calibration fixture to a noise level that is 10^{-2} times the energy of the light that is Rayleigh scattered into the density sensor's monochromator system at 100 km by the following technique·

1. Minimizing the fields of view (FOV) of the collimating and focal mirrors using the aperture stops $A_{s,1}$, $A_{s,2}$, $A_{D,1}$ and $A_{D,2}$ and the straight edges $A_{s,o}$ and $A_{D,o}$ as shown in Figure V.

2. Trapping the FOV of the collimating and focal mirrors at some point beyond their point of separation in separate Rayleigh horns as illustrated in Figures IV and V.

3. Stopping the source's collimated beam with a total of nine aperture stops to reduce the level of energy diffracted onto $A_{D,o}$ and the generation of stray light by diffraction from $A_{s,1}$ and $A_{s,2}$ and reflection from the walls of the fixture.

4. Placing aperture stops $A_{D,3}$, $A_{D,4}$, ..., $A_{D,9}$ in the focal mirror's FOV to attenuate the energy level of stray light entering $A_{D,1}$ off axis to the FOV of the focal mirror by multiple reflections between the aperture stops.

5. Supplementing the aperture stop $A_{s,k}$ and $A_{D,q}$ where k = 1, 2, ..., 9 and q = 1, 2, ..., 9 with stops a_s and a_D that serve as additional reflecting surfaces to assist in the attenuation of stray light. Figure V shows the general location of these stops. Their number and spacing must be determined experimentally in the calibration fixture.

6. Separate the source's aperture stops $A_{s,k}$ and a_s from the detector's $A_{D,q}$ and a_D by a partition extending from the interface of the calibration fixture to the point of intersection of $A_{s,1}$ and $A_{D,1}$.

7. Sharpen the edges of the aperture stops $A_{s,k}$ and $A_{D,q}$ where, k = 0, 1, 2, ..., 9 and q = 0, 1, 2, ..., 9 and the common edge of the light traps T_s and T_D.

8. Coat the interior of the fixture and all its components with a paint having a reflectance that is not greater than 0.05 in the wavelength region of 1800 to 2800 A and a vapor pressure lower than 10^{-4} torr.

The assumption that the scattering of unwanted stray light by the fused silica exit window is negligible is reasonably valid since its contribution is less than 10% of the collimating mirrors. In the event that the optical quality of the exit window renders it a larger contributor, the energy level of its stray light will be attenuated by multiple reflections in the Rayleigh horn light traps and the interior of the fixture, however, the apertures of the light traps may have to be enlarged to include the FOV of the window which is slightly larger than the collimating mirrors as can be seen in Figure V.

5.0 APPENDIX I

Figure VII is an illustration of the Cornu spiral, which can be constructed from the Fresnel integrals

$$X = \int_0^v \cos\left(\frac{\pi}{2} t^2\right) dt$$

and A-I

$$Y = \int_0^v \sin\left(\frac{\pi}{2} t^2\right) dt$$

X and Y are the coordinates of a point located on the spiral an arc distance v from the origin where, v is positive if measured from the origin along that portion of the spiral which lies in the third quadrant. A complete discussion of the integrals A-I are contained in several references.[2,6,7] Evaluating them for large values of v requires evaluating the integrals of the $\cos\left(\frac{\pi}{2} t^2\right)$ and the $\sin\left(\frac{\pi}{2} t^2\right)$ expanded in a power series.

For large values of v, the integrals may be evaluated from the following series[7] which is in inverse powers of v;

$$X = \frac{1}{2} - \frac{1}{\pi v}\left[P(v) \cos\left(\frac{\pi}{2} v^2\right) - Q(v) \sin\left(\frac{\pi}{2} v^2\right)\right]$$

and A-II.

$$Y = \frac{1}{2} - \frac{1}{\pi v}\left[P(v) \sin\left(\frac{\pi}{2} v^2\right) - Q(v) \cos\left(\frac{\pi}{2} v^2\right)\right]$$

where,

$$Q(v) = 1 - \frac{1\text{-}3}{(\pi v^2)^2} + \frac{1\text{-}3\text{-}5\text{-}7}{(\pi v^2)^4} - \cdots$$

A-III.

$$P(v) = \frac{1}{\pi v^2} - \frac{1\text{-}3\text{-}5}{(\pi v^2)^3} + \frac{1\text{-}3\text{-}4\text{-}7\text{-}9}{(\pi v^2)^5} - \cdots$$

The relative intensity of a point on a screen where v was evaluated using XXII

$$v = \frac{fy}{f+h}\sqrt{\frac{2(f+h)}{fh}} \qquad \text{XXII}$$

is given by

$$(I/I_o) = 1/2\left[(1/2 + X)^2 + (1/2 + y)^2\right]$$

for positive values of v.

Table I gives values of Q(v), P(v), x, y and I/I_o for arc lengths v from 6 to 200 in eight significant figures.

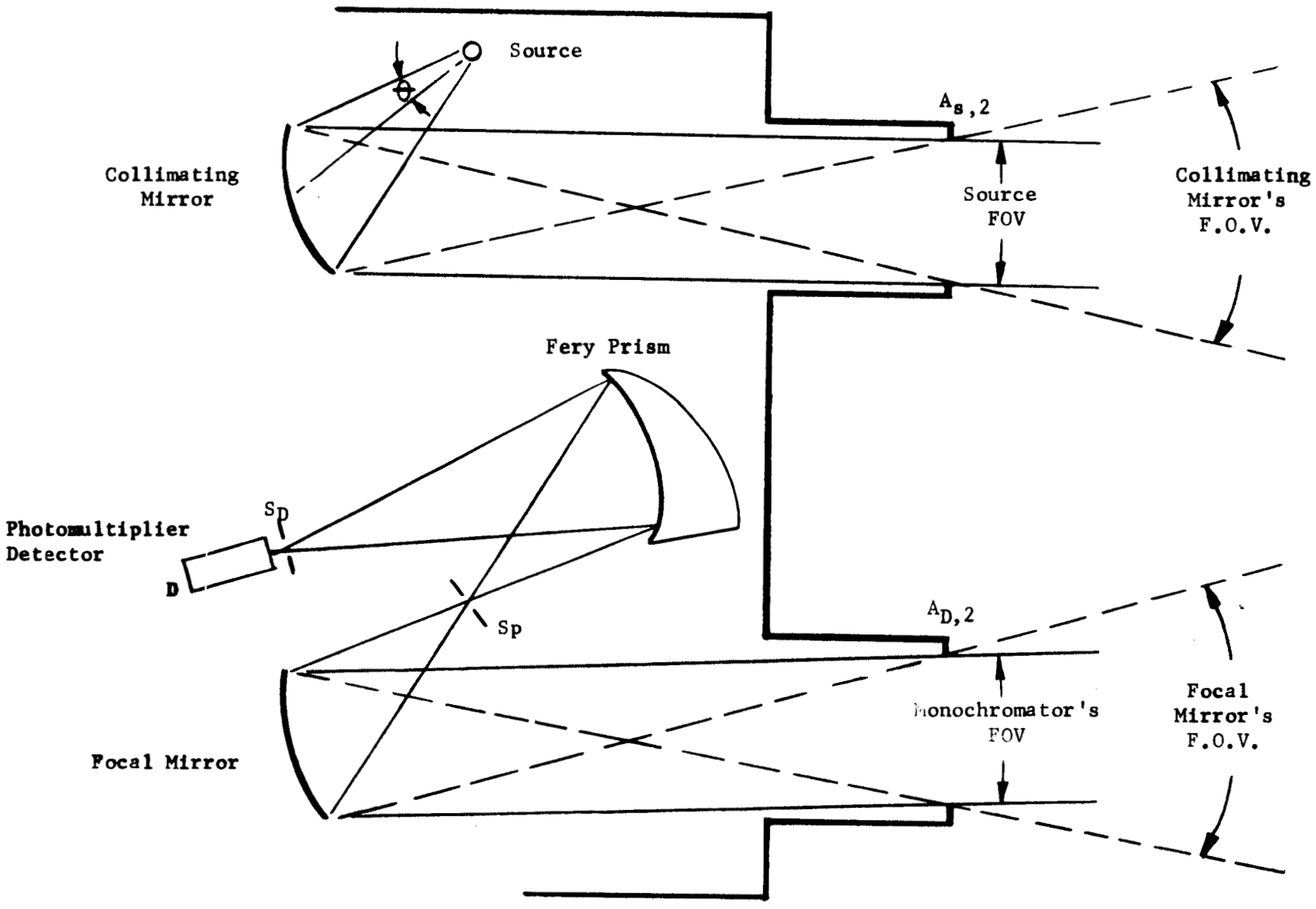

FIGURE I

Optical Diagram of the Ultraviolet Density Sensor

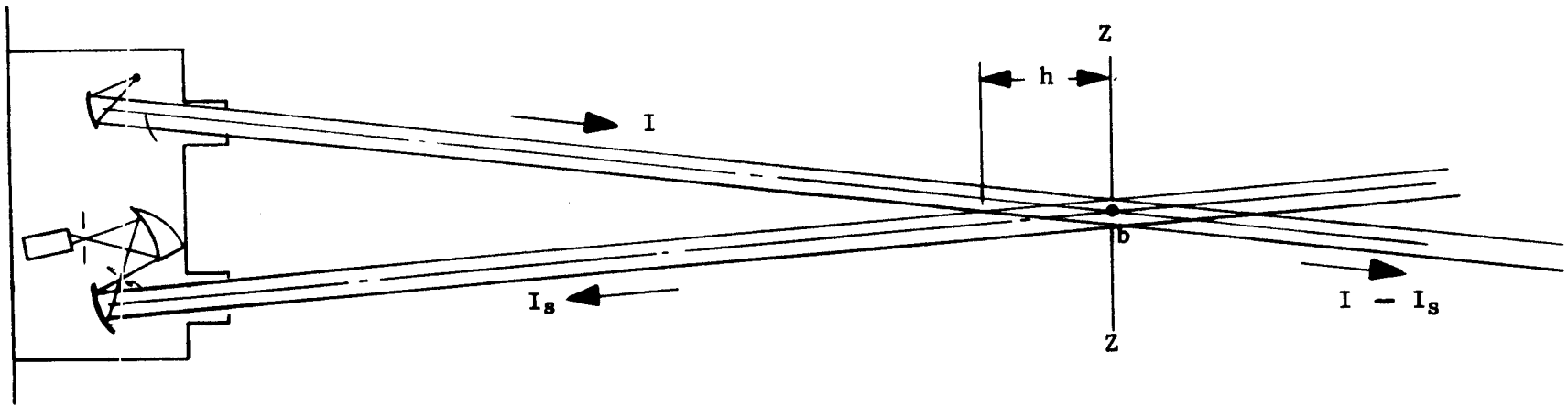

Z-Z Scattering Zone

FIGURE II

Optical Paths of the Source's Collimated
Light I and the Collimated Rayleigh Scattered Light I_s

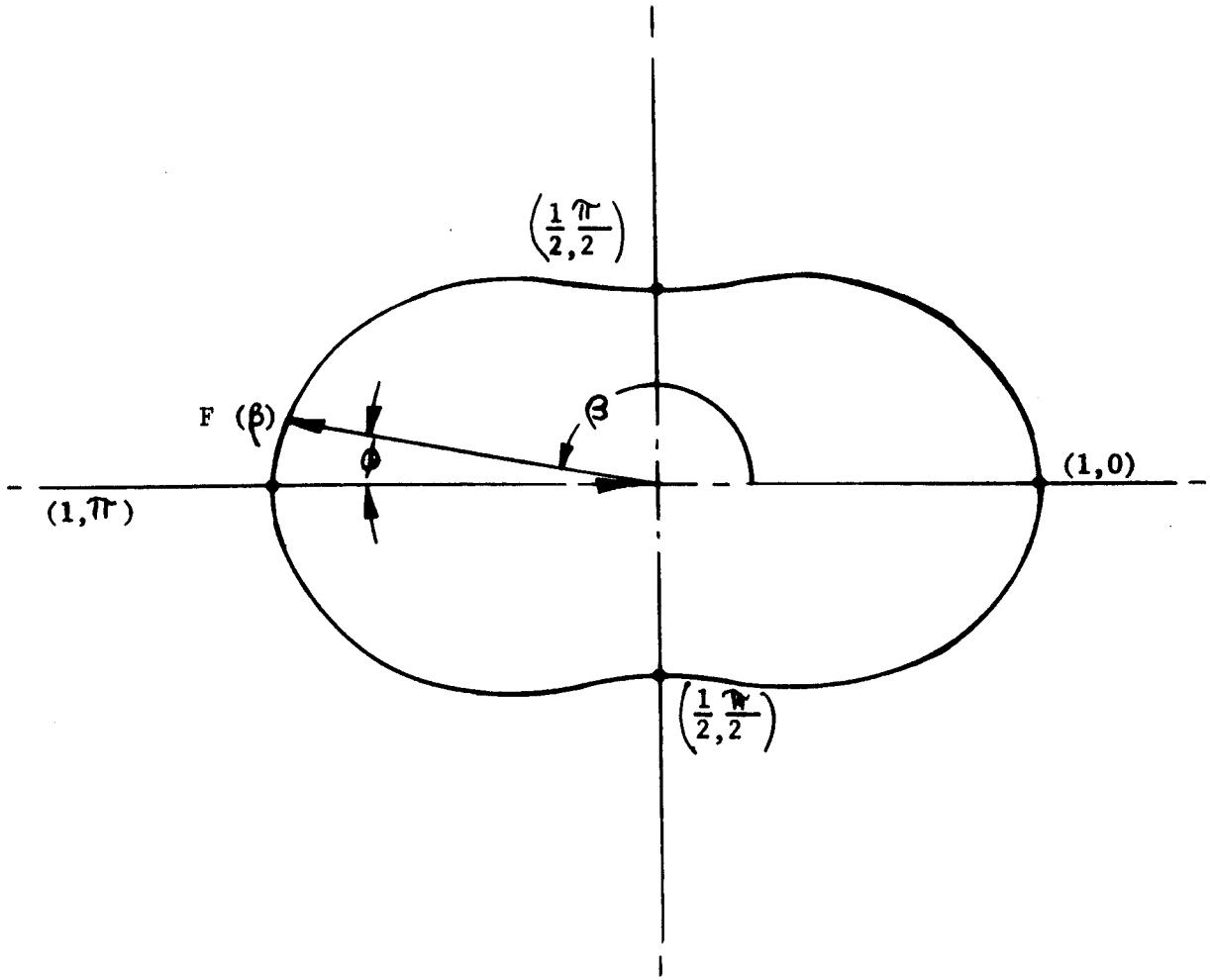

FIGURE III

Intensity Distribution F(β) of Light Rayleigh Scattered where,

$$F(\beta) = 1/2\ (1 + \cos^2\beta)$$

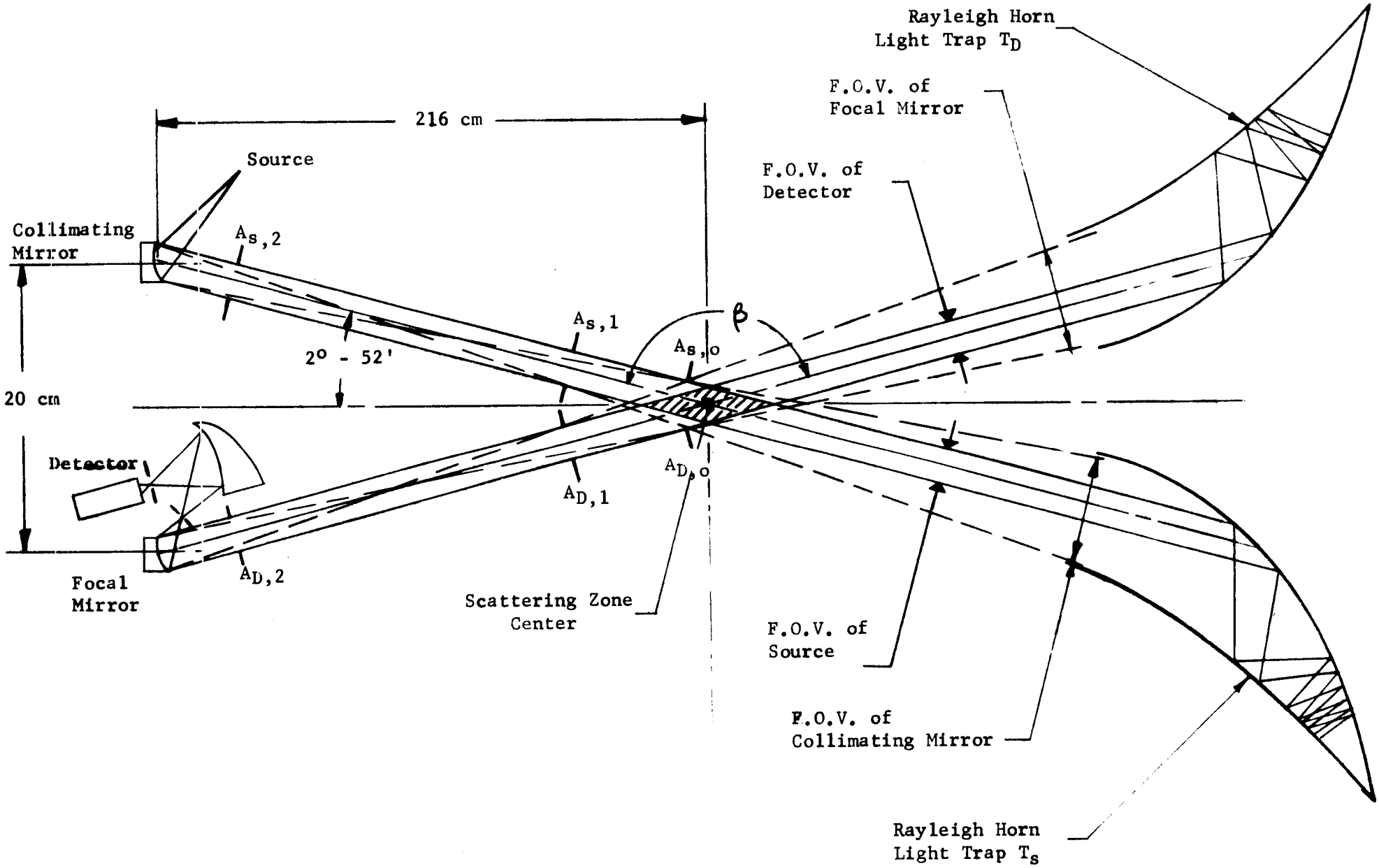

FIGURE IV

Optical Path of the Ultraviolet Density Sensor

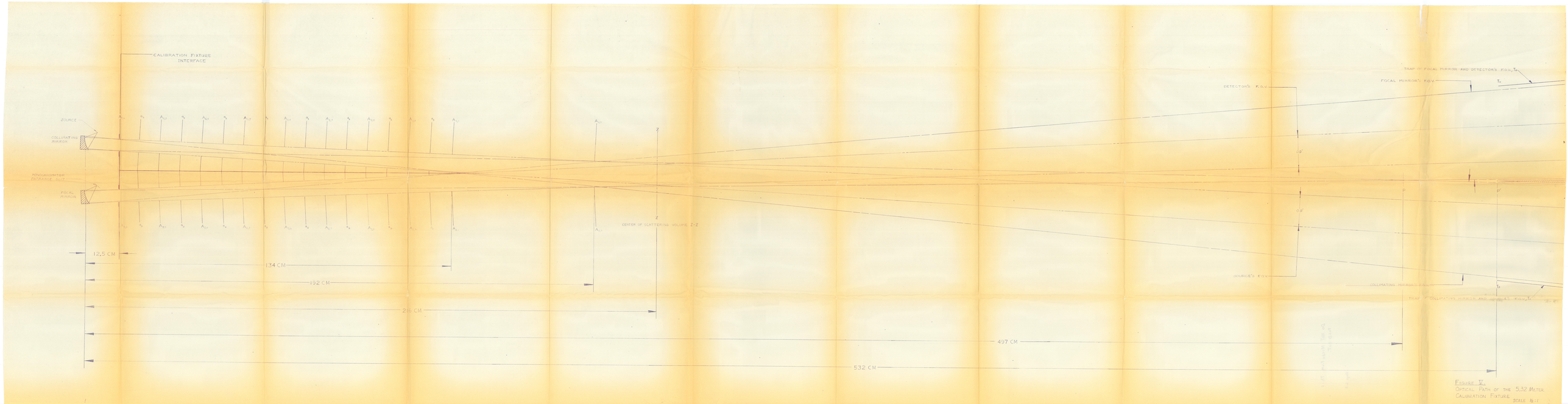

FIGURE V.
OPTICAL PATH OF THE 5.32 METER CALIBRATION FIXTURE
SCALE 1/8:1

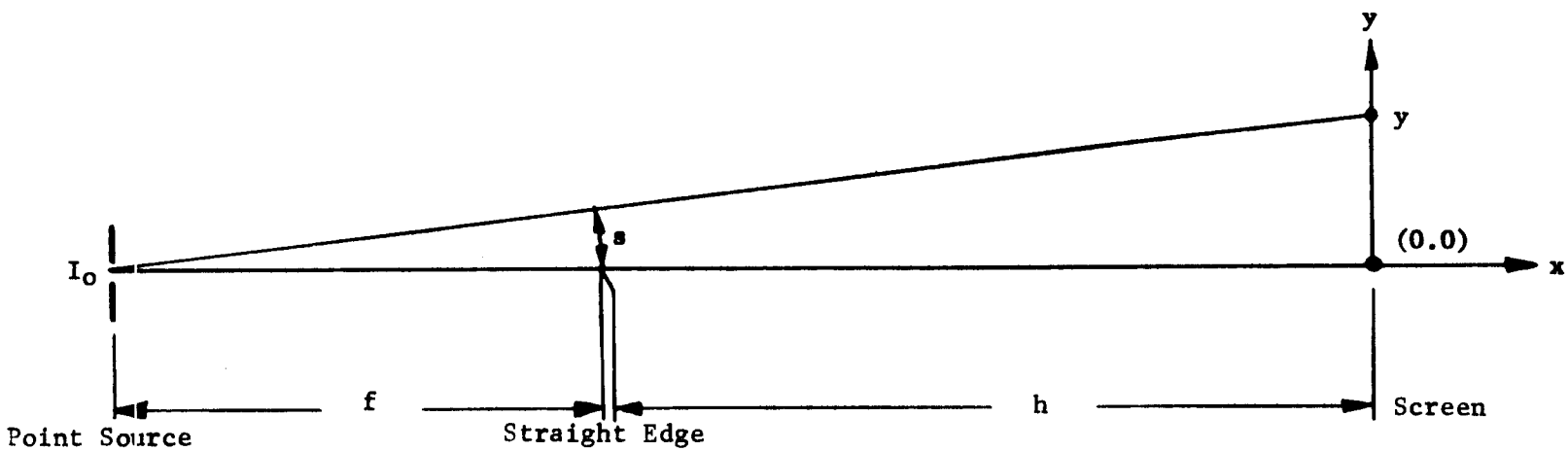

FIGURE VI

Fresnel Diffraction From A Straight Edge

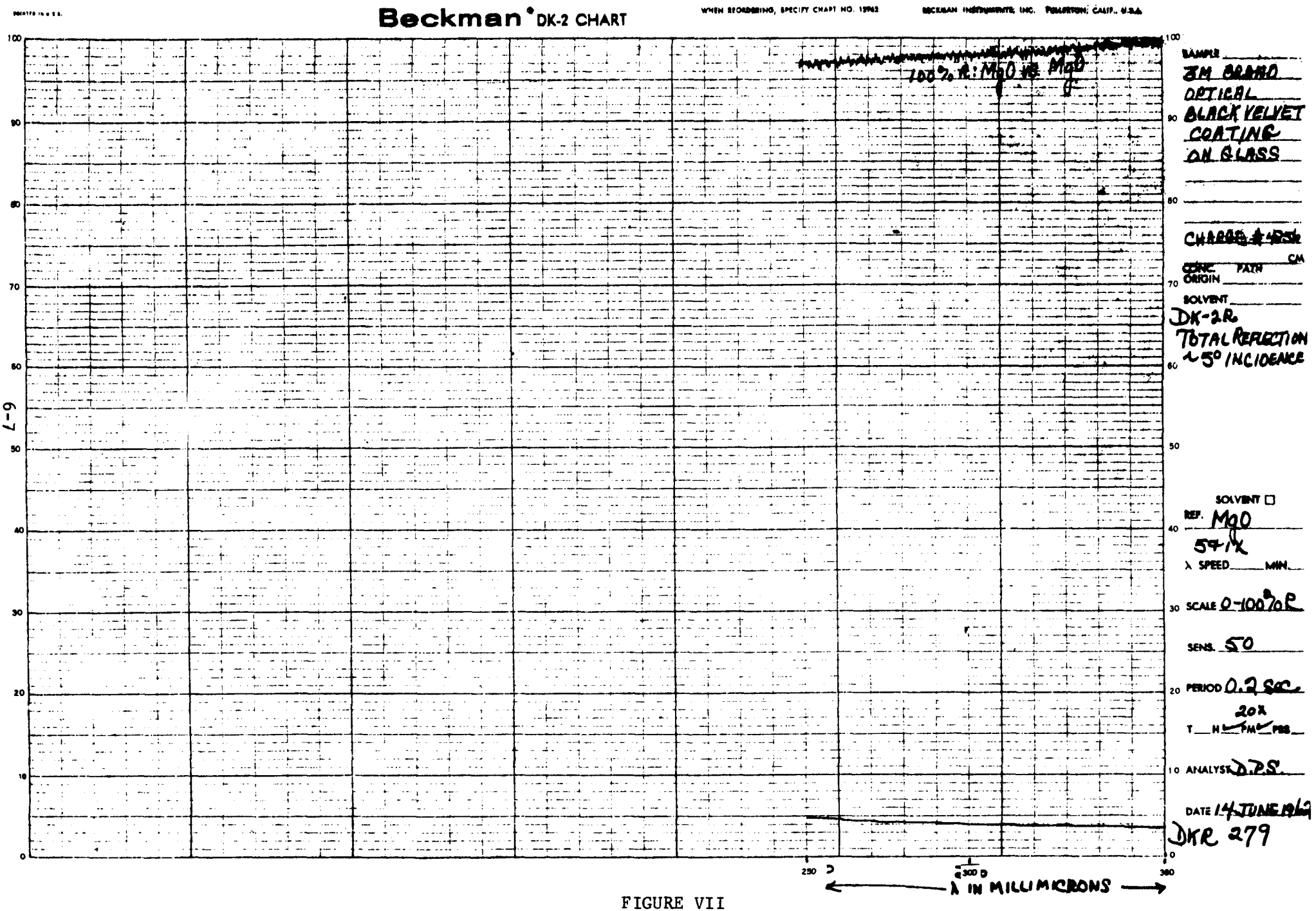
Beckman DK-2 CHART
WHEN REORDERING, SPECIFY CHART NO. 12962
BECKMAN INSTRUMENTS, INC. FULLERTON, CALIF., U.S.A.
100% R: MgO vs MgO
SAMPLE
3M BRAND
OPTICAL
BLACK VELVET
COATING
ON GLASS
CHARGE
CONC. PATH CM
ORIGIN
SOLVENT
DK-2R
TOTAL REFLECTION
~5° INCIDENCE
SOLVENT
REF. MgO
54%
λ SPEED MIN.
SCALE 0-100% R
SENS. 50
PERIOD 0.2 SEC.
20%
T H FM PBS
ANALYST D.P.S.
DATE 14 JUNE 1962
DKR 279
λ IN MILLIMICRONS
250
300
380
L-9

FIGURE VII

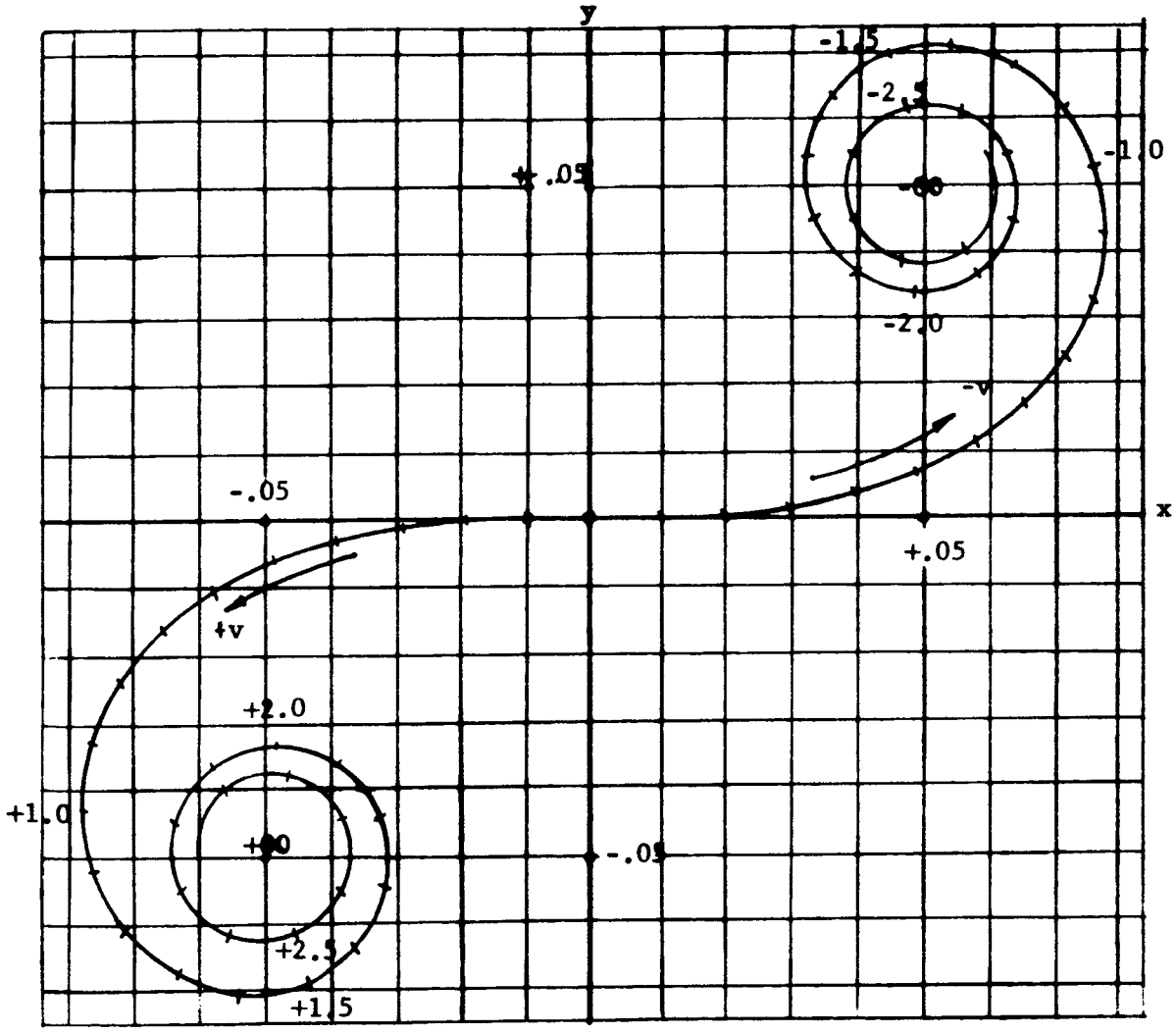

FIGURE VIII

Cornu Spiral

BIBLIOGRAPHY

1. Spectral Emission of Argon for AED AF 40(600)-1033, Giannini Scientific Corp. (received October 1964).

2. Handbook of Physics 6-124, Condon & Odishaw, McGraw Hill Book Co., Inc. 1958.

3. J.O.S.A. 47,176 (1957) Rudolf Penndorf, Tables of the Refractive Index for Standard Air and the Rayleigh Scattering Coefficient for the Spectral Region between 0.2 and 20.0 u and Their Application to Atmospheric Optics.

4. ARDC Model Atmosphere 1959, Geophysics Research Directorate, Air Force Cambridge Research Center (quoted from private communication with N.A.S.A. Edwards).

5. Handbook of Geophysics, U. S. Air Force, Macmillan 1960.

6. Fundamentals of Optics, Francis A. Jenkins and Harvey E. White, 3rd Ed. McGraw Hill Book Co., Inc. 1957.

7. Principles of Optics, Max Born and Emil Wolf, 2nd Ed. A Pergamon Press Book, Macmillan Co., N. Y. 1964.

TABLE I

v × 10^n	n	Q(v) × 10^n	n	P(v) × 10^n	n	X × 10	Y × 10	(Z/10) × 10^n	n
6.0000000E	00	9.9976614E-01		8.8316233E-03		4.9953133E-01	4.4696077E-01	1.4066897E-03	
7.0000000E	00	9.9987368E-01		6.4320190E-03		5.4546709E-01	4.9770479E-01	1.0336716E-03	
8.0000000E	00	9.9992586E-01		4.9717493E-03		4.9980199E-01	4.6021422E-01	7.9147370E-04	
9.0000000E	00	9.9995372E-01		3.9298422E-03		5.3536612E-01	4.9986096E-01	6.2539085E-04	
1.0000000E	01	9.9996971E-01		3.1826154E-03		4.9989861E-01	4.6816998E-01	5.0658015E-04	
1.1000000E	01	9.9997930E-01		2.6303873E-03		5.2893666E-01	4.9992373E-01	4.1866805E-04	
1.2000000E	01	9.9998540E-01		2.2103233E-03		4.9994135E-01	4.7347457E-01	3.5180093E-04	
1.3000000E	01	9.9998940E-01		1.8833902E-03		5.2448511E-01	4.9995391E-01	2.9976136E-04	
1.4000000E	01	9.9999210E-01		1.6239658E-03		4.9996308E-01	4.7726376E-01	2.5846898E-04	
1.5000000E	01	9.9999400E-01		1.4146681E-03		5.2122053E-01	4.9996991E-01	2.2515589E-04	
1.6000000E	01	9.9999540E-01		1.2433691E-03		4.9997528E-01	4.8010573E-01	1.9789129E-04	
1.7000000E	01	9.9999640E-01		1.1013982E-03		5.1872404E-01	4.9997941E-01	1.7529504E-04	
1.8000000E	01	9.9999720E-01		9.8242371E-04		4.9998246E-01	4.8231617E-01	1.5635907E-04	
1.9000000E	01	9.9999770E-01		8.8173459E-04		5.1675311E-01	4.9998483E-01	1.4033346E-04	
2.0000000E	01	9.9999820E-01		7.9576720E-04		4.9998685E-01	4.8408454E-01	1.2665101E-04	
2.1000000E	01	9.9999850E-01		7.2178551E-04		5.1515759E-01	4.9998861E-01	1.1487617E-04	
2.2000000E	01	9.9999880E-01		6.5766081E-04		4.9999017E-01	4.8553139E-01	1.0467038E-04	
2.3000000E	01	9.9999900E-01		6.0171675E-04		5.1383954E-01	4.9999158E-01	9.5766465E-05	
2.4000000E	01	9.9999910E-01		5.5261892E-04		4.9999222E-01	4.8673711E-01	8.7952155E-05	
2.5000000E	01	9.9999930E-01		5.0929394E-04		5.1273238E-01	4.9999347E-01	8.1056770E-05	
2.6000000E	01	9.9999940E-01		4.7087106E-04		4.9999403E-01	4.8775733E-01	7.4941495E-05	
2.7000000E	01	9.9999950E-01		4.3663784E-04		5.1178924E-01	4.9999459E-01	6.9493095E-05	
2.8000000E	01	9.9999960E-01		4.0600651E-04		4.9999516E-01	4.8863180E-01	6.4617995E-05	
2.9000000E	01	9.9999960E-01		3.7848895E-04		5.1097619E-01	4.9999573E-01	6.0238375E-05	
3.0000000E	01	9.9999970E-01		3.5367698E-04		4.9999632E-01	4.8938968E-01	5.6289450E-05	
3.1000000E	01	9.9999970E-01		3.3122723E-04		5.1026805E-01	4.9999588E-01	5.2716430E-05	
3.2000000E	01	9.9999980E-01		3.1084904E-04		4.9999653E-01	4.9005282E-01	4.9473200E-05	
3.3000000E	01	9.9999980E-01		2.9229520E-04		5.0964575E-01	4.9999719E-01	4.6520250E-05	
3.4000000E	01	9.9999980E-01		2.7535426E-04		4.9999692E-01	4.9063795E-01	4.3823994E-05	
3.5000000E	01	9.9999980E-01		2.5984454E-04		5.0909466E-01	4.9999764E-01	4.1355513E-05	
3.6000000E	01	9.9999990E-01		2.4560925E-04		4.9999748E-01	4.9115806E-01	3.9089954E-05	
3.7000000E	01	9.9999990E-01		2.3251251E-04		5.0860296E-01	4.9999825E-01	3.7005461E-05	
3.8000000E	01	9.9999990E-01		2.2043604E-04		4.9999819E-01	4.9162343E-01	3.5083463E-05	
3.9000000E	01	9.9999990E-01		2.0927659E-04		5.0816179E-01	4.9999879E-01	3.3307409E-05	
4.0000000E	01	9.9999990E-01		1.9894356E-04		4.9999824E-01	4.9204226E-01	3.1662814E-05	
4.1000000E	01	9.9999990E-01		1.8935735E-04		5.0776365E-01	4.9999934E-01	3.0137131E-05	
4.2000000E	01	1.0000000E	00	1.8044769E-04		4.9999848E-01	4.9242120E-01	2.8719105E-05	
4.3000000E	01	1.0000000E	00	1.7215238E-04		5.0740255E-01	4.9999867E-01	2.7398874E-05	
4.4000000E	01	1.0000000E	00	1.6441520E-04		4.9999890E-01	4.9276569E-01	2.6167621E-05	
4.5000000E	01	1.0000000E	00	1.5719001E-04		5.0707355E-01	4.9999916E-01	2.5017554E-05	
4.6000000E	01	1.0000000E	00	1.5042995E-04		4.9999877E-01	4.9308022E-01	2.3941678E-05	
4.7000000E	01	1.0000000E	00	1.4409678E-04		5.0677255E-01	4.9999912E-01	2.2933716E-05	
4.8000000E	01	1.0000000E	00	1.3815530E-04		4.9999894E-01	4.9336855E-01	2.1988065E-05	
4.9000000E	01	1.0000000E	00	1.3257394E-04		5.0649612E-01	4.9999927E-01	2.1099787E-05	
5.0000000E	01	1.0000000E	00	1.2732372E-04		4.9999909E-01	4.9363381E-01	2.0264187E-05	
5.1000000E	01	1.0000000E	00	1.2237978E-04		5.0624137E-01	4.9999958E-01	1.9477349E-05	
5.2000000E	01	1.0000000E	00	1.1771313E-04		4.9999948E-01	4.9387866E-01	1.8735401E-05	
5.3000000E	01	1.0000000E	00	1.1331794E-04		5.0600584E-01	4.9999943E-01	1.8035057E-05	
5.4000000E	01	1.0000000E	00	1.0915975E-04		4.9999943E-01	4.9410538E-01	1.7373272E-05	
5.5000000E	01	1.0000000E	00	1.0522639E-04		5.0578745E-01	4.9999946E-01	1.6747289E-05	
5.6000000E	01	1.0000000E	00	1.0150196E-04		4.9999954E-01	4.9431590E-01	1.6154496E-05	
5.7000000E	01	1.0000000E	00	7.7971439E-05		5.0558438E-01	4.9999797E-01	1.5592651E-05	
5.8000000E	01	1.0000000E	00	9.4622433E-05		4.9999760E-01	4.9451190E-01	1.5059623E-05	
5.9000000E	01	1.0000000E	00	9.1442070E-05		5.0549508E-01	4.9999944E-01	1.4553444E-05	
6.0000000E	01	1.0000000E	00	8.8419407E-05		4.9999807E-01	4.9469484E-01	1.4072362E-05	
6.1000000E	01	1.0000000E	00	8.5544170E-05		5.0521819E-01	4.9999887E-01	1.3614753E-05	
6.2000000E	01	1.0000000E	00	8.2806935E-05		4.9999917E-01	4.9486597E-01	1.3179132E-05	
6.3000000E	01	1.0000000E	00	8.0199008E-05		5.0505253E-01	4.9999899E-01	1.2764030E-05	
6.4000000E	01	1.0000000E	00	7.7712370E-05		4.9999835E-01	4.9502641E-01	1.2368299E-05	
6.5000000E	01	1.0000000E	00	7.5339611E-05		5.0489707E-01	4.9999973E-01	1.1990647E-05	
6.6000000E	01	1.0000000E	00	7.3073993E-05		4.9999821E-01	4.9517713E-01	1.1630039E-05	
6.7000000E	01	1.0000000E	00	7.0908860E-05		5.0475089E-01	4.9999867E-01	1.1285478E-05	
6.8000000E	01	1.0000000E	00	6.8838641E-05		4.9999868E-01	4.9531898E-01	1.0955974E-05	
6.9000000E	01	1.0000000E	00	6.6857777E-05		5.0461318E-01	4.9999826E-01	1.0640716E-05	
7.0000000E	01	1.0000000E	00	6.4961137E-05		4.9999970E-01	4.9545112E-01	[illegible]	

7.1400000E C1	1.0000000E 00	6.3144174E-05	5.0448823E-01	4.9999845E-01	1.0704867E-06
7.2000000E C1	1.0000000E 00	6.1402359E-05	4.9999903E-01	4.9557903E-01	9.7784476E-06
7.3000000E C1	1.0000000E 00	5.9731637E-05	5.0436040E-01	4.9999920E-01	9.5065440E-06
7.4000000E C1	1.0000000E 00	5.8128174E-05	4.9999896E-01	4.9569852E-01	9.2511655E-06
7.5000000E C1	1.0000000E 00	5.6584624E-05	5.0424413E-01	4.9999933E-01	9.0063205E-06
7.6000000E C1	1.0000000E 00	5.5109050E-05	4.9999942E-01	4.9581172E-01	8.7709445E-06
7.7000000E C1	1.0000000E 00	5.3686340E-05	5.0413389E-01	5.0000010E-01	8.5445230E-06
7.8000000E C1	1.0000000E 00	5.2331174E-05	4.9999835E-01	4.9591911E-01	8.3268325E-06
7.9000000E C1	1.0000000E 00	5.1030245E-05	5.0402924E-01	5.0000029E-01	8.1173470E-06
8.0000000E C1	1.0000000E 00	4.9775918E-05	4.9999607E-01	4.9602113E-01	7.9157030E-06
8.1000000E C1	1.0000000E 00	4.8515452E-05	5.0392575E-01	4.9999668E-01	7.7214730E-06
8.2000000E C1	1.0000000E 00	4.7334353E-05	4.9999910E-01	4.9611818E-01	7.5342630E-06
8.3000000E C1	1.0000000E 00	4.6205527E-05	5.0383505E-01	5.0000060E-01	7.3538040E-06
8.4000000E C1	1.0000000E 00	4.5119943E-05	4.9999291E-01	4.9671060E-01	7.1777800E-06
8.5000000E C1	1.0000000E 00	4.4056730E-05	5.0374482E-01	5.0000059E-01	7.0119380E-06
8.6000000E C1	1.0000000E 00	4.3039112E-05	4.9999916E-01	4.9629873E-01	6.8469975E-06
8.7000000E C1	1.0000000E 00	4.2054416E-05	5.0365873E-01	5.0000059E-01	6.6931525E-06
8.8000000E C1	1.0000000E 00	4.1104055E-05	4.9999919E-01	4.9638285E-01	6.5418870E-06
8.9000000E C1	1.0000000E 00	4.0185568E-05	5.0357651E-01	4.9999701E-01	6.3957155E-06
9.0000000E C1	1.0000000E 00	3.9297517E-05	4.9999921E-01	4.9546323E-01	6.2543710E-06
9.1000000E C1	1.0000000E 00	3.8438580E-05	5.0349791E-01	5.0000057E-01	6.1176870E-06
9.2000000E C1	1.0000000E 00	3.7607501E-05	4.9999923E-01	4.9654011E-01	5.9854190E-06
9.3000000E C1	1.0000000E 00	3.6803085E-05	5.0342268E-01	5.0000057E-01	5.8573690E-06
9.4000000E C1	1.0000000E 00	3.6024205E-05	4.9999926E-01	4.9661374E-01	5.7334120E-06
9.5000000E C1	1.0000000E 00	3.5259723E-05	5.0335063E-01	5.0000056E-01	5.6133605E-06
9.6000000E C1	1.0000000E 00	3.4519833E-05	5.0000258E-01	4.9668428E-01	5.4970025E-06
9.7000000E C1	1.0000000E 00	3.3803353E-05	5.0328154E-01	4.9999728E-01	5.3842555E-06
9.8000000E C1	1.0000000E 00	3.3103469E-05	5.0000253E-01	4.9675195E-01	5.2749170E-06
9.9000000E C1	1.0000000E 00	3.2477285E-05	5.0321525E-01	5.0000055E-01	5.1689160E-06
1.0000000E C2	1.0000000E 00	3.1830938E-05	4.9999931E-01	4.9681691E-01	5.0660305E-06
1.0100000E C2	1.0000000E 00	3.1203732E-05	5.0315158E-01	5.0000054E-01	4.9662283E-06
1.0200000E C2	1.0000000E 00	3.0594952E-05	4.9999934E-01	4.9687932E-01	4.8693220E-06
1.0300000E C2	1.0000000E 00	3.0003760E-05	5.0309038E-01	5.0000053E-01	4.7752243E-06
1.0400000E C2	1.0000000E 00	2.9429538E-05	4.9999935E-01	4.9693933E-01	4.6838506E-06
1.0500000E C2	1.0000000E 00	2.8871645E-05	5.0303152E-01	5.0000052E-01	4.5950568E-06
1.0600000E C2	1.0000000E 00	2.8329466E-05	4.9999936E-01	4.9699708E-01	4.5087644E-06
1.0700000E C2	1.0000000E 00	2.7802413E-05	5.0297485E-01	5.0000052E-01	4.4249663E-06
1.0800000E C2	1.0000000E 00	2.7289942E-05	4.9999938E-01	4.9705269E-01	4.3433182E-06
1.0900000E C2	1.0000000E 00	2.6791506E-05	5.0292027E-01	5.0000051E-01	4.2639885E-06
1.1000000E C2	1.0000000E 00	2.6306602E-05	4.9999939E-01	4.9710628E-01	4.1868078E-06
1.1100000E C2	1.0000000E 00	2.5834744E-05	5.0286765E-01	4.9999765E-01	4.1117110E-06
1.1200000E C2	1.0000000E 00	2.5375469E-05	4.9999941E-01	4.9715795E-01	4.0386242E-06
1.1300000E C2	1.0000000E 00	2.4929332E-05	5.0281690E-01	5.0000050E-01	3.9674629E-06
1.1400000E C2	1.0000000E 00	2.4492012E-05	4.9999942E-01	4.9720781E-01	3.8981626E-06
1.1500000E C2	1.0000000E 00	2.4068808E-05	5.0276791E-01	5.0000049E-01	3.8306629E-06
1.1600000E C2	1.0000000E 00	2.3655609E-05	4.9999943E-01	4.9725595E-01	3.7649053E-06
1.1700000E C2	1.0000000E 00	2.3252368E-05	5.0272059E-01	5.0000049E-01	3.7009050E-06
1.1800000E C2	1.0000000E 00	2.2860520E-05	4.9999944E-01	4.9730246E-01	3.6383611E-06
1.1900000E C2	1.0000000E 00	2.2477374E-05	5.0267487E-01	5.0000048E-01	3.5774649E-06
1.2000000E C2	1.0000000E 00	2.2104853E-05	4.9999945E-01	4.9734742E-01	3.5180904E-06
1.2100000E C2	1.0000000E 00	2.1740933E-05	5.0263066E-01	5.0000047E-01	3.4601861E-06
1.2200000E C2	1.0000000E 00	2.1386044E-05	4.9999947E-01	4.9739091E-01	3.4036754E-06
1.2300000E C2	1.0000000E 00	2.1039717E-05	5.0258788E-01	4.9999789E-01	3.3485636E-06
1.2400000E C2	1.0000000E 00	2.0701735E-05	4.9999948E-01	4.9743299E-01	3.2947702E-06
1.2500000E C2	1.0000000E 00	2.0371832E-05	5.0254647E-01	4.9999793E-01	3.2422568E-06
1.2600000E C2	1.0000000E 00	2.0049753E-05	4.9999949E-01	4.9747374E-01	3.1909946E-06
1.2700000E C2	1.0000000E 00	1.9735252E-05	5.0250679E-01	5.0000046E-01	3.1409453E-06
1.2800000E C2	1.0000000E 00	1.9428093E-05	4.9999950E-01	4.9751321E-01	3.0920623E-06
1.2900000E C2	1.0000000E 00	1.9128050E-05	5.0246751E-01	5.0000045E-01	3.0443023E-06
1.3000000E C2	1.0000000E 00	1.8834904E-05	4.9999951E-01	4.9755147E-01	2.9976496E-06
1.3100000E C2	1.0000000E 00	1.8548446E-05	5.0242984E-01	5.0000044E-01	2.9520612E-06
1.3200000E C2	1.0000000E 00	1.8268473E-05	4.9999951E-01	4.9758857E-01	2.9074974E-06
1.3300000E C2	1.0000000E 00	1.7994732E-05	5.0239303E-01	5.0000044E-01	2.8639424E-06
1.3400000E C2	1.0000000E 00	1.7727215E-05	4.9999952E-01	4.9762456E-01	2.8213576E-06
1.3500000E C2	1.0000000E 00	1.7465563E-05	5.0235785E-01	5.0000043E-01	2.7797283E-06
1.3600000E C2	1.0000000E 00	1.7209608E-05	4.9999953E-01	4.9765949E-01	2.7389936E-06
1.3700000E C2	1.0000000E 00	1.6959341E-05	5.0232342E-01	5.0000043E-01	2.6991402E-06
1.3800000E C2	1.0000000E 00	1.6714444E-05	4.9999954E-01	4.9769316E-01	2.6601780E-06
1.3900000E C2	1.0000000E 00	1.6474814E-05	5.0228903E-01	[illegible]	[illegible]

2

1.40000000E 02	1.00000000E 00	1.6240000E-05	4.9999955E-01	4.9772635E-01	2.5867185E-06
1.41000000E 02	1.00000000E 00	1.6010759E-05	5.0225751E-01	5.0000042E-01	2.5481757E-06
1.42000000E 02	1.00000000E 00	1.5786065E-05	4.9944955E-01	4.9775939E-01	2.5124077E-06
1.43000000E 02	1.00000000E 00	1.5566036E-05	5.0222594E-01	5.0000041E-01	2.4774044E-06
1.44000000E 02	1.00000000E 00	1.5350592E-05	5.0001176E-01	4.9778952E-01	2.4431124E-06
1.45000000E 02	1.00000000E 00	1.5139952E-05	5.0219524E-01	5.0000041E-01	2.4095393E-06
1.46000000E 02	1.00000000E 00	1.4932908E-05	4.9999957E-01	4.9781980E-01	2.3766360E-06
1.47000000E 02	1.00000000E 00	1.4729431E-05	5.0216537E-01	5.0000040E-01	2.3444135E-06
1.48000000E 02	1.00000000E 00	1.4530043E-05	4.9999958E-01	4.9784926E-01	2.3128413E-06
1.49000000E 02	1.00000000E 00	1.4337637E-05	5.0213630E-01	5.0000040E-01	2.2818888E-06
1.50000000E 02	1.00000000E 00	1.4147105E-05	4.9999958E-01	4.9787794E-01	2.2515693E-06
1.51000000E 02	1.00000000E 00	1.3960347E-05	5.0210401E-01	5.0000039E-01	2.2218531E-06
1.52000000E 02	1.00000000E 00	1.3777264E-05	4.9999959E-01	4.9790596E-01	2.1927112E-06
1.53000000E 02	1.00000000E 00	1.3597755E-05	5.0208045E-01	5.0000039E-01	2.1641361E-06
1.54000000E 02	1.00000000E 00	1.3421735E-05	4.9999959E-01	4.9793306E-01	2.1361205E-06
1.55000000E 02	1.00000000E 00	1.3249110E-05	5.0205361E-01	5.0000039E-01	2.1086570E-06
1.56000000E 02	1.00000000E 00	1.3079774E-05	4.9999960E-01	4.9795956E-01	2.0816977E-06
1.57000000E 02	1.00000000E 00	1.2913703E-05	5.0202745E-01	5.0000038E-01	2.0552768E-06
1.58000000E 02	1.00000000E 00	1.2750756E-05	5.0000161E-01	4.9798539E-01	2.0293279E-06
1.59000000E 02	1.00000000E 00	1.2590873E-05	5.0200194E-01	5.0000038E-01	2.0038849E-06
1.60000000E 02	1.00000000E 00	1.2433979E-05	4.9999961E-01	4.9801057E-01	1.9789159E-06
1.61000000E 02	1.00000000E 00	1.2280006E-05	5.0197709E-01	5.0000037E-01	1.9544227E-06
1.62000000E 02	1.00000000E 00	1.2128863E-05	4.9999962E-01	4.9803513E-01	1.9303571E-06
1.63000000E 02	1.00000000E 00	1.1980499E-05	5.0195282E-01	5.0000037E-01	1.9067530E-06
1.64000000E 02	1.00000000E 00	1.1834840E-05	4.9999962E-01	4.9805909E-01	1.8835658E-06
1.65000000E 02	1.00000000E 00	1.1691873E-05	5.0192815E-01	5.0000037E-01	1.8608099E-06
1.66000000E 02	1.00000000E 00	1.1551342E-05	4.9999963E-01	4.9808248E-01	1.8384155E-06
1.67000000E 02	1.00000000E 00	1.1413456E-05	5.0190604E-01	5.0000036E-01	1.8164942E-06
1.68000000E 02	1.00000000E 00	1.1277986E-05	5.0000152E-01	4.9810530E-01	1.7949451E-06
1.69000000E 02	1.00000000E 00	1.1144913E-05	5.0188349E-01	5.0000036E-01	1.7737673E-06
1.70000000E 02	1.00000000E 00	1.1014182E-05	4.9999964E-01	4.9812759E-01	1.7529596E-06
1.71000000E 02	1.00000000E 00	1.0885738E-05	5.0185146E-01	5.0000035E-01	1.7325167E-06
1.72000000E 02	1.00000000E 00	1.0759529E-05	4.9999964E-01	4.9814937E-01	1.7124157E-06
1.73000000E 02	1.00000000E 00	1.0635503E-05	5.0183564E-01	4.9999852E-01	1.6926906E-06
1.74000000E 02	1.00000000E 00	1.0513634E-05	4.9999965E-01	4.9817064E-01	1.6732790E-06
1.75000000E 02	1.00000000E 00	1.0393792E-05	5.0181891E-01	5.0000035E-01	1.6542168E-06
1.76000000E 02	1.00000000E 00	1.0276016E-05	4.9999965E-01	4.9819143E-01	1.6354627E-06
1.77000000E 02	1.00000000E 00	1.0160231E-05	5.0179836E-01	4.9999855E-01	1.6170503E-06
1.78000000E 02	1.00000000E 00	1.0046391E-05	4.9999966E-01	4.9821175E-01	1.5989190E-06
1.79000000E 02	1.00000000E 00	9.9344554E-06	5.0177826E-01	4.9999857E-01	1.5811053E-06
1.80000000E 02	1.00000000E 00	9.8241793E-06	4.9999799E-01	4.9823162E-01	1.5635861E-06
1.81000000E 02	1.00000000E 00	9.7161239E-06	5.0175860E-01	4.9799331E-01	1.5463593E-06
1.82000000E 02	1.00000000E 00	9.6096456E-06	4.9999442E-01	4.9825106E-01	1.5294111E-06
1.83000000E 02	1.00000000E 00	9.5049092E-06	5.0173938E-01	4.9999339E-01	1.5127431E-06
1.84000000E 02	1.00000000E 00	9.4018752E-06	4.9999794E-01	4.9827006E-01	1.4963483E-06
1.85000000E 02	1.00000000E 00	9.3005078E-06	5.0172059E-01	5.0000033E-01	1.4802150E-06
1.86000000E 02	1.00000000E 00	9.2007713E-06	4.9999967E-01	4.9828866E-01	1.4643423E-06
1.87000000E 02	1.00000000E 00	9.1026307E-06	5.0170218E-01	4.9999693E-01	1.4487130E-06
1.88000000E 02	1.00000000E 00	9.0060515E-06	4.9999798E-01	4.9830687E-01	1.4333465E-06
1.89000000E 02	1.00000000E 00	8.9110016E-06	5.0168417E-01	4.9999865E-01	1.4182151E-06
1.90000000E 02	1.00000000E 00	8.8174487E-06	4.9999465E-01	4.9832470E-01	1.4033293E-06
1.91000000E 02	1.00000000E 00	8.7253608E-06	5.0166654E-01	4.9999866E-01	1.3886786E-06
1.92000000E 02	1.00000000E 00	8.6347084E-06	4.9999803E-01	4.9834214E-01	1.3742517E-06
1.93000000E 02	1.00000000E 00	8.5454615E-06	5.0164926E-01	4.9999538E-01	1.3600399E-06
1.94000000E 02	1.00000000E 00	8.4575985E-06	4.9999805E-01	4.9835923E-01	1.3460649E-06
1.95000000E 02	1.00000000E 00	8.3710687E-06	5.0163235E-01	4.9999869E-01	1.3322841E-06
1.96000000E 02	1.00000000E 00	8.2859677E-06	4.9999864E-01	4.9837598E-01	1.3187267E-06
1.97000000E 02	1.00000000E 00	8.2019645E-06	5.0161578E-01	5.0000031E-01	1.3053725E-06
1.98000000E 02	1.00000000E 00	8.1193155E-06	5.0000129E-01	4.9839238E-01	1.2922218E-06
1.99000000E 02	1.00000000E 00	8.0379255E-06	5.0159954E-01	4.9990872E-01	1.2792849E-06
2.00000000E 02	1.00000000E 00	7.9577473E-06	4.9999492E-01	4.9840466E-01	1.2665126E-06

3